Examensarbete

Algorithmic Construction of Fundamental Polygons for Certain Fuchsian Groups

David Larsson

LiTH - MAT - EX - - 2015/05 - - SE

Algorithmic Construction of Fundamental Polygons for Certain Fuchsian Groups

Mathematics and Applied Mathematics, Linköpings Universitet

David Larsson

LiTH - MAT - EX - - 2015/05 - - SE

Examensarbete: **30 hp**

Level: **A**

Supervisor: **Antonio F. Costa**,
Departamento de Matemáticas Fundamentales,
Universidad Nacional de Educación a Distancia

Examiner: **Milagros Izquierdo**,
Mathematics and Applied Mathematics,
Linköpings Universitet

Linköping: **June 2015**

Abstract

The work of mathematical giants, such as Lobachevsky, Gauss, Riemann, Klein and Poincaré, to name a few, lies at the foundation of the study of the highly structured Riemann surfaces, which allow definition of holomorphic maps, corresponding to analytic maps in the theory of complex analysis. A topological result of Poincaré states that every path-connected Riemann surface can be realised by a construction of identifying congruent points in the complex plane, the Riemann sphere or the hyperbolic plane; just three simply connected surfaces that cover the underlying Riemann surface. This requires the discontinuous action of a discrete subgroup of the automorphisms of the corresponding space. In the hyperbolic plane, which is the richest source for Riemann surfaces, these groups are called Fuchsian, and there are several ways to study the action of such groups geometrically by computing fundamental domains. What is accomplished in this thesis is a combination of the methods found by Reidemeister & Schreier, Singerman and Voight, and thus provides a unified way of finding Dirichlet domains for subgroups of cofinite groups with a given index. Several examples are considered in-depth.

Keywords: Compact Riemann surfaces and uniformization; Fuchsian groups and automorphic functions; Hyperbolic geometry; Topological groups; Permutation groups; Computational methods; Covering spaces, branched coverings; Generators, relations, and presentations

URL for electronic version:

http://urn.kb.se/resolve?urn=urn:nbn:se:liu:diva-119916

Populärvetenskaplig sammanfattning

Några av de stora matematiker som har lagt grunden för de djupt strukturerade Riemannytorna är Lobachevsky, Gauss, Riemann, Klein och Poincaré. Dessa ytor tillåter oss att generalisera analytiska funktioner, kända från komplex analys, till holomorfa avbildningar. Ett av Poincarés topologiska resultat om dessa ytor är att varje sammanhängande Riemannyta kan realiseras genom att identifiera punkter i en av tre ytor: det komplexa planet,

Riemannsfären eller det hyperboliska planet. Alla tre är dessutom enkelt sammanhängande och övertäcker genom denna operation den underliggande Riemannytan. Operationen innebär att en diskret undergrupp till ytans automorfismgrupp tillåts verka på ytan. Det hyperboliska planet ger upphov till de allra flesta Riemannytor och motsvarande grupper kallas i detta fall för fuchsiska. För att studera dessa grupper och deras verkan geometriskt beräknas ofta fundamentalpolygoner. Vår uppsats bidrar med en kombination av metoder som upptäckts av Reidemeister och Schreier, Singerman och Voight, för att på så sätt ge en enhetlig bild av hur Dirichletpolygoner kan beräknas för undergrupper, med ett givet index, till kofinita grupper. Flera exempel betraktas ingående.

Acknowledgements

Standing on the shoulders of giants, I first of all want to posthumously thank all the pioneers of this fascinating subject.

Secondly, an enormous thanks to my supervisor, Antonio F. Costa, who provided much needed help throughout the process and averted several possible embarassments. The same extends to my examiner, Milagros Izquierdo, who invested much time in setting up the thesis in cooperation with Antonio and also in helping me to understand David Singerman's method and otherwise was of enormous help in spotting errors and perfecting the text as it now stands.

My opponent, Caroline Granfeldt, took a very serious approach to studying the thesis and without her opposition I could not have finished the work in time.

Furthermore, I want to thank my wife, Lydia, for her unending support and for bearing with me during this thesis and even more during the process leading up to this climax. I want to thank my three wonderful children, Johannes, Maria and Teresa, for helping me to keep my eyes on the ultimate trophy and not attach myself too much to earthly things.

I thank all my friends, who have provided much needed "whitespace" for my mind to work on. You know who you are!

Finally, but all the more important, I thank the heavenly court, most especially the Blessed Virgin Mary and Blessed Faá di Bruno, for their intercession for me and the success of my mathematical studies.

Symbols

Most of the reoccurring symbols that are not presumed to be known by the reader or have differing notation in the literature are described here.

$\mathcal{A}$	Surface atlases are in calligraphic style.
$\mathrm{Aut}(X)$	The automorphism group of the space X.
δA	Boundary of the set A.
$\overline{A}$	Closure of the set $A \subset X$ in X.
$\overline{\overline{A}}$	Closure of the set $A \subset X$ in $\overline{X}$.
$\overline{z}$	Complex conjugate of the complex number z.
$\chi(G)$	Euler characteristic of a group G.
$[\alpha, \beta]$	Geodesic between α and β.
$G, H, \ldots$	Groups are denoted by capital letters starting with G.
μ	Hyperbolic area.
ρ	Hyperbolic norm and metric in $\mathfrak{U}$.
ρ^*	Hyperbolic norm and metric in $\mathfrak{D}$.
e	Identity element in a group.
$[G : H]$	Index of H, as a subgroup of G.
I_g	Isometric circle associated to the Möbius transformation g.
$\mathring{A}$	Interior of the set A.
$\ker(\theta)$	Kernel of the map θ.
Ω	Lattice in $\mathbb{C}$.
Γ	The modular group.
$g,\ h,\ s,\ t$	Möbius transformations are denoted by small letters in this order.
$G \cdot x$	Orbit of x under G.
$\langle \mathcal{E} \vert \mathcal{R} \rangle$	Presentation for some group.
r	Reduction map.
Σ	The Riemann sphere.
$\mathrm{pairs}(F)$	Side-pairing of a fundamental polygon F.
$\mathrm{sign}(G)$	Signature of the Fuchsian group G.
$\mathrm{Stab}_G(x)$	Stabiliser of x in G.
$\mathfrak{U}$	Upper half-plane model of the hyperbolic plane.
$\mathfrak{D}$	Unit disc model of the hyperbolic plane.

List of Figures

List of Tables

List of algorithms

Contents

Chapter 1

Introduction

Consider the vectors in the lattice displayed in Figure 1.1. The way integer translations by these vectors act in the plane can be described by considering a fundamental domain for the lattice, which is graphically represented as the grey area. With this domain the correspondence between algebra and geometry becomes clear, since the algebraic quotient $\mathbb{C}/\Omega$ corresponds to the topological construction of pasting the opposing sides of the quadrilateral.

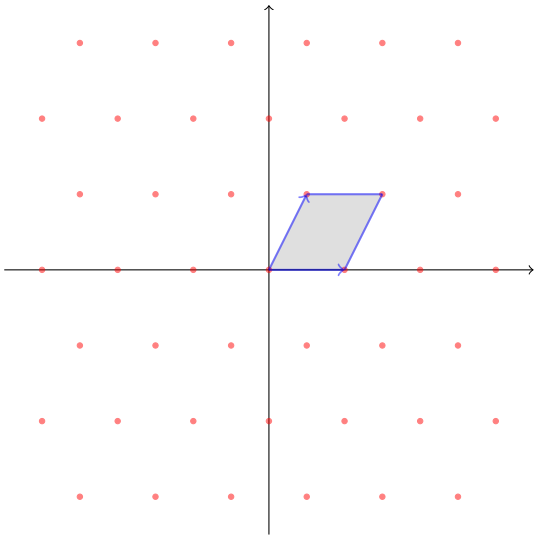

Figure 1.1: *Fundamental domain for a lattice.*

However, this example covers only one of the cases which are interesting in the study of Riemann surfaces, i.e., surfaces with a complex structure that makes it possible to generalise analytic functions of one complex variable. In fact, only the torus arises in this way. The other special case is the sphere, and otherwise all compact surfaces are obtained by quotients, "pastings", of the hyperbolic plane. Finding fundamental domains for the corresponding groups, i.e., Fuchsian groups, is non-trivial, but in a lot of interesting cases

it is possible to employ an algorithm which ends in finite time, using only the generators of the group.

The three main objectives of this thesis is thus to: 1. explain the theory of compact Riemann surfaces, Fuchsian groups and hyperbolic geometry; 2. use a known structure of subgroups of Fuchsian groups to compute signatures and generators for certain subgroups of the modular group Γ; and 3. show how to construct an algorithm to compute Dirichlet/Ford fundamental domains, and apply it to the modular group and some of its subgroups.

More specifically, we make the following claims:

1. All compact Riemann surfaces with genus 2 or more[1] are realised as quotient spaces of the hyperbolic plane by a Fuchsian group, which can be reduced to the quotient of a *fundamental domain* of the same group. This realisation can be seen by pasting the sides of a polygon in the hyperbolic plane. In Chapter 3 we paste the sides of a few Euclidean polygons and of a hyperbolic triangle. This further introduces us to the topic of signatures and presentations.

2. Given knowledge of a Fuchsian group's signature, there is a permutation representation of its index N subgroups that allows us to find the signatures of subgroups of index N by considering the cycle decomposition of the images of generators. This theorem was discovered by David Singerman and is explained in Section 3.4. We use it to find all the index 2 and 3 subgroups of the modular group, as well as one particular index 6 subgroup, in Section 5.2 through Section 5.5. By using the Reidemeister-Schreier algorithm, also explained in Section 3.4, we are able to find the generators for these subgroups, making explicit what is only implicit in the theorem of Singerman.

3. The problem of finding fundamental domains is in general a highly non-trivial task, but we explain how, given certain restrictions on the Fuchsian group G, there is a halting algorithm, discovered by John Voight, that produces a fundamental domain for G in Section 4.3. This algorithm is then applied to the modular group and to the mentioned subgroups of the modular group in Chapter 5, yielding Dirichlet/Ford domains for the groups.

[1] This can temporarily be thought of as "handles" on the surface.

1.1 Historical Background

> There is no branch of mathematics, however abstract, which may not some day be applied to phenomena of the real world.
> —Nikolai Lobachevsky, [3, p. 572]

This thesis is placed in the intersection of three areas, which have had parallel courses in history, but with considerable overlap. The intersection of geometry, both Euclidean and not, with complex function theory and group theory, has yielded and continues to yield much fruit. The connecting point is Riemann surfaces.

We begin the story with the discovery of non-Euclidean geometry, summarised from [3, p. 585-590]. This was one of the most revolutionary discoveries in geometry and was independently arrived at by three mathematicians: Nikolai Ivanovitch Lobachevsky (1793–1856), Carl Friedrich Gauss (1777–1855) and János Bolyai (1802–1860). The one who is credited with most of the development of the theory is Lobachevsky, who published his works on what he called "imaginary geometry" in 1829. Even though Gauss had been working on the same problem in about the same time as Lobachevsky and arrived at similar conclusions regarding the famous fifth, or parallel, postulate of Euclid (∼300 B.C.), he had not published any of his results and refrained from doing so, even if he was quietly endorsing both Lobachevsky and Bolyai. The independent work of Bolyai was mainly obscured by his own disappointment in not receiving priority in the discovery, which lead to him abandoning the pursuit altogether. Thus, the field was open for Lobachevsky. The discovery he, and the other two, had made was that Euclid's postulate that any line has a unique non-intersecting line through a point not on that line could be replaced without losing logical consistency. The work was made concrete by instead using the postulate that any line had infinitely many non-intersecting lines through a point not on the line. The astonishment that was felt by everyone, including the discoverers themselves, can be garnered from the term that Lobachevsky had used for this type of geometry.

Another leap forward was made by Georg Friedrich Bernhard Riemann (1826–1866) in two steps. First he published his doctoral thesis on complex functions of one variable, introducing Riemann surfaces as a way of visualising the multiple-valued functions appearing in complex analysis, such as the complex logarithm. Later, as a step in his academic career, he was required to hold a lecture, his *Habilitation*, which introduced the notions of higher-dimensional equivalents of surfaces, which he called manifolds, and also generalised differential geometry by noticing that the metric associated to Euclidean geometry was only one of many metrics. He went even further and connected the Gaussian curvature of a surface to the metric. This connection gives one way of distinguishing three, in one sense "basic",

geometries:

- the Euclidean plane, with constant Gaussian curvature 0;
- the sphere, with constant Gaussian curvature 1;
- the hyperbolic plane, with constant Gaussian curvature -1.

The work was further generalised by Adolf Hurwitz (1859–1919), who first considered Riemann surfaces as branched covering surfaces of the Riemann sphere, in [10].

Building on the work of Riemann, Eugenio Beltrami (1835–1900) was the first to give a model for Lobachevskian, or hyperbolic, geometry with the pseudo-sphere, giving a way to visualise hyperbolic geometry, which had up until this time been researched in axiomatic terms. Furthermore, he thus gave hyperbolic geometry an equal footing with Euclidean geometry and by the pseudo-sphere it inherited its geometry from its Euclidean cousin. This was to be followed by models by Felix Klein (1849–1925) and Henri Poincaré (1854–1912), [3, p. 580, 591–594, 650–654]. The former is perhaps most famous for his *Erlanger Programm*, wherein he showed how to use group theory in conjunction with geometry and thereby distinguishing geometries by certain invariants under group action. One part of this was showing how Euclidean geometry was a special case of affine geometry, which in turn was a special case of projective geometry. Klein showed this via linear fractional transformations, also known as Möbius transformations, after the mathematician August Ferdinand Möbius (1790–1860) who had studied them extensively earlier. The latter of the two, Poincaré, had done his doctoral thesis on existence theorems for differential equations, which included properties of automorphic functions, which are meromorphic[2] complex functions invariant under a countable group of Möbius transformations. He was the one who insisted on the name Fuchsian groups, since they characterise the functions he considered in this dissertation, which were Fuchsian functions, while Klein wanted to name them Schwartzian. Poincaré was regarded as a universal mathematician, taking on a wide variety of areas. Among the more noteworthy in regards to our thesis is his work in establishing much of the foundations for algebraic topology. Even though work had been done in this area earlier, it is widely recognised that Poincaré's work on *analysis situs*, as it was called, was a starting point for the much wider and deeper interest that emerged during the 20th century.

Another character that we encounter in this story [3, p. 662, 668] is Hermann Weyl (1885–1955), who also worked in this field and in a 1913 lecture on Riemann surfaces had emphasised the abstract nature of the 2-manifolds which bore the name of Riemann surfaces.

[2] Analytic except for poles.

A revival of interest in the area at hand was to come in the 1960s, when Alexander Murray MacBeath (1923–2014) and his students started using combinatorial methods to study Fuchsian groups and Riemann surfaces. Notable among them is David Singerman which has influenced this thesis immensely, by inheritance.

The work done in this area is vast and there are many other characters that could be mentioned. Thus, the above is a brief overview of the centuries-old roots of the current thesis.

Chapter 2

Basic Concepts

Given the nature of a master thesis, we aim to be as self-contained as possible, thus reiterating concepts that may already have been encountered. Moreover, it is useful to fix notation even for basic concepts. Thus, we will walk through some of the prerequisites for understanding this thesis.

2.1 Group Theory

The first concept we need to deal with is that of a group. Even though this concept took time to develop, its mature form is fairly straight-forward in its basic concepts. Employing these basic notions has proven to be a very fruitful and challenging area of ongoing research.

Recall that a group $(G, \cdot)$ is a set G accompanied by the operation $\cdot$, that satisfies the following properties, see [9, p. 13],

(i) *Associativity:* $x \cdot (y \cdot z) = (x \cdot y) \cdot z$ for all choices of $x, y, z \in G$;

(ii) *Existence of an identity:* There is a unique element $e \in G$ such that $e \cdot g = g \cdot e = g$ for all $g \in G$;

(iii) *Existence of inverse:* For every $x \in G$, there is an inverse $x^{-1} \in G$ such that $x \cdot x^{-1} = x^{-1} \cdot x = e$.

Remark 2.1. We will almost everywhere[1] abbreviate $x \cdot y$ as xy. In the case of a commutative group operation $\cdot$ is often denoted by $+$. The identity in this case will be denoted 0.

Permutation groups hold a special place in our thesis, so we define a *permutation* as a bijective function on a finite set of symbols X, see [9, p. 107-110]. In this thesis we will always take the symbol set as contiguous

[1] The set of places where we write out $\cdot$ is even finite!

positive integers starting at 1, so $X = \{1, 2, \ldots, n\}$. This bijection can be represented in several ways. First, by explicitly giving the bijection, as

$$\begin{pmatrix} 1 & 2 & 3 & 4 & 5 \\ 2 & 3 & 1 & 4 & 5 \end{pmatrix},$$

which means that 1 maps to 2, which maps to 3, which maps back to 1, while 4 and 5 remain fixed.

This illustrates that there is a more convenient way to represent this permutation. The canonical decomposition of the permutation into disjoint cycles is then written as

$$(1, 2, 3)(4)(5),$$

where we get both the orbit of each element under the permutation as well as the order of the mapping of elements.

Multiplication of permutations is then most easily described by an example, from which the reader can infer the general pattern, recalling that the first permutation to be applied is the one on the right,

$$(1, 2)(1, 3, 2) = (1, 3)(2),$$
$$(1, 3, 2)(1, 2) = (1)(2, 3).$$

The first line shows that 1 maps to 3 by the first permutation and then 3 is not altered by the second. Then, 3 maps to 2 by the first which is mapped to 1 by the second and 2 remains fixed after applying both permutations.

Needing to make transitions between groups, we introduce certain maps between groups, see [9, p. 98-99, 102]. First, let $G,\ H$ be groups. A *group homomorphism* $\theta : G \to H$ is such that for every $g,\ h \in G$,

$$\theta(g^{-1}) = \theta(g)^{-1} \text{ and } \theta(gh) = \theta(g)\theta(h).$$

A *group isomorphism* is a bijective homomorphism and an *epimorphism* is a surjective homomorphism. Moreover, a *group automorphism* is an isomorphism of a group with itself, which need not be the identity. The *kernel* of a homomorphism is the pre-image of the unit element

$$\ker(\theta) = \theta^{-1}(\{e\}).$$

Moreover, some subsets and subgroups of G are particularly interesting, see [8, p. 55]. Let G be a group acting on X. Then, the *stabiliser* of a point $x \in X$ is the subgroup

$$\mathrm{Stab}_G(x) = \{g \in G : g(x) = x\}.$$

Moreover, the *orbit* of a point $x \in X$ under G is the set

$$G \cdot x = \{y \in X : \exists g \in G : g(x) = y\},$$

i.e., all the points reached from x by elements in G. As an example, the group generated by $(1,2,3)(4)(5)$ consists of only three elements, all fixing 4 and 5. Thus, the orbit of 4 and 5 under this group is simply $\{4\}$ and $\{5\}$, while for 1, 2 and 3 their common orbit will be $\{1,2,3\}$.

Let $H \leq G$ be groups. A *conjugation*, [9, p. 126], of $h \in H$ by $g \in G$ is the element

$$ghg^{-1} \in G,$$

with its *conjugacy class* being the equivalence class of all possible conjugations of h by g in G.

A conjugation of the subgroup H by g is the subgroup

$$gHg^{-1} = \{s \in G : s = ghg^{-1},\ h \in H\} \leq G.$$

Finally, if a subgroup $H \leq G$ has n left cosets in G, which means that H splits G into n equivalence classes, it is said to be of index $[G : H] = n$, see [8, p. 16].

2.2 Topology

A brief recapitulation of topological notions is also warranted, and the definitions in this section are taken from Jones & Singerman [13, p. 167-172] and Munkres [15, p. 76, 98, 137-139].

The main tools in the topological toolbox we will use are covering spaces. In order for this to make sense, we start at the beginning.

Definition 2.1. Let X be a set and $\tau \subset \mathcal{P}(X)$. The ordered pair (X, τ), often abbreviated X, is a *topological space* if

(i) $\varnothing,\ X \in \tau$.

(ii) Let Λ be an arbitrary index set. If, for every $\lambda \in \Lambda$, $A_\lambda \in \tau$, then the union $\bigcup_{\lambda\in\Lambda} A_\lambda \in \tau$.

(iii) If $A, B \in \tau$, then $A \cap B \in \tau$.

The sets in τ are called *open* and their complements are called *closed*.

Remark 2.2. Let X be a universal set. We fix the following notation: $\mathring{D}$ is the interior of D, i.e., the maximal open subset of D. Further, $D^c = X \setminus D$ is the complement of D. In the following, we will also use $\overline{D}$ for the closure of D in X, i.e., the minimal closed superset of D and $\overline{\overline{D}}$ for the closure of D in $\overline{X}$. Finally, we denote the boundary by $\delta D = \overline{D} \setminus \mathring{D}$.

A space in and of itself is not so interesting, unless we have operations that we can use on them. The main tool in comparing topological spaces

is *homeomorphism*[2], which is an open, continuous bijection between two spaces. Imagine that you can move between the spaces in the sense that you can continuously deform one into the other. To be more precise, a mapping p is *open* if it maps open sets to open sets, and *continuous* if every point in the image of p has an open neighbourhood such that its pre-image is open in the domain of p. Furthermore, $p : X \to Y$ is a bijection if every point in the domain gets mapped to at most one point in Y and every point in Y has a non-empty pre-image. This extends also to subsets of X and Y, in the following definition.

Definition 2.2. Let X, Y be topological spaces. Two open sets $U \subset X$ and $V \subset Y$ are *homeomorphic* if there is a homeomorphism between U and V.

In terms of our thesis, the most interesting form of topology is that of a surface. Using these topological terms, the extension of the definition to higher dimensional equivalents of surfaces, called n-manifolds, is nowadays easy[3]. The theory surrounding higher-dimensional geometry is far from easy, however.

Definition 2.3. A *surface*, or 2-manifold, is a Hausdorff topological space S, such that for every point $s \in S$, there is an open set $U \ni s$ that is homeomorphic to an open subset $V \subset \mathbb{R}^2$.

The importance of the constraint that S is a Hausdorff space might be more apparent if this is understood to mean that our notion of what can be said of distinct points in Euclidean space is also true of surfaces. This restriction means that we require the topology of S be such that any two, distinct, points s_1, s_2 can be separated by open sets, i.e., there are open neighbourhoods $S_1 \ni s_1$ and $S_2 \ni s_2$ such that $S_1 \cap S_2 = \varnothing$. See Figure 2.1.

In order to find ourselves around a surface, we need some sense of where we are. The analogous terms that are employed in the definitions of coordinate systems on surfaces should be kept in mind.

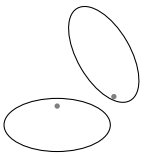

Figure 2.1: *Two distinct points can be separated by open sets in Hausdorff spaces.*

Definition 2.4. Let S be a surface. A *chart* for, not necessarily all of, S is an ordered pair (U, ϕ), such that ϕ is a homeomorphism between $U \subset S$ and $\phi(U) \subset \mathbb{R}^2$. An *atlas* for S is a set of charts, $\mathcal{A}$, such that $S = \bigcup_{(U,\phi)\in\mathcal{A}} U$ and moreover, if $S \supset U \cap V \neq \varnothing$, with charts (U, ϕ) and (V, ψ), we define the *coordinate transition functions* as $\phi \circ \psi^{-1} : \psi(U \cap V) \to \phi(U \cap V)$ (and its inverse). The definition is illustrated in Figure 2.2.

[2]Not to be confused with homomorphism.

[3]The historical development of this notion shows that this was not always the case.

There are two special examples of surfaces that we will give here.

Example 2.1. Any plane in $\mathbb{R}^3$ is a surface with the above definition, since it can be homeomorphically transformed by rotations and translations to a plane with coordinates of the form $(x_1, x_2, 0)$, which is easily identified with $\mathbb{R}^2$.

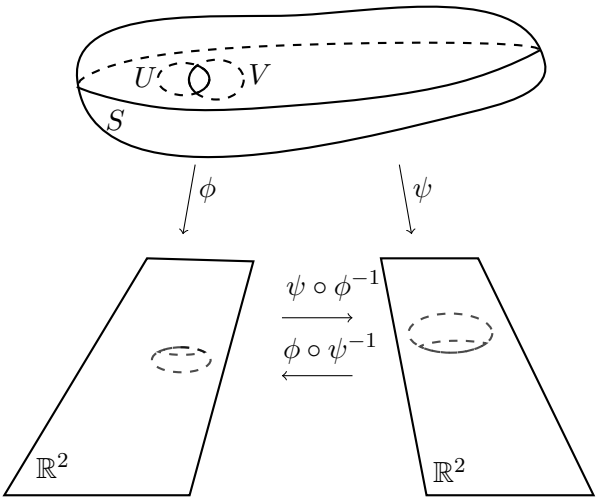

Figure 2.2: *An atlas with a pair of overlapping charts with coordinate transition functions.*

Example 2.2. The sphere $\{(x, y, z) \in \mathbb{R}^3 : x^2 + y^2 + z^2 = 1\}$ is a surface. This is shown by using stereographic projection of the punctured sphere from the north pole $(0, 0, 1)$ as one chart and the stereographic projection of the punctured sphere from the south pole $(0, 0, -1)$ as the other chart, with coordinate transition function a rotation by π around the x-axis.

One important definition, that will be needed in Section 2.3, is that a topological space X is said to be *path-connected*, or *connected*, if for any two points $x, y \in X$, there is a continuous map $\gamma : [0, 1] \to X$ with $\gamma(0) = x$ and $\gamma(1) = y$.

Moreover, we will make frequent use of the quotient construction, mentioned briefly in Chapter 1.

Definition 2.5. [15, p. 137] Let X, Y be topological spaces. Then, a surjective map $p : X \to Y$ is said to be a *quotient map* if $U \subseteq Y$ is open in Y if, and only if, $p^{-1}(U)$ is open in X.

Definition 2.6. [15, p. 138] Let X be a topological space, A a set, $p : X \to A$ a surjective map. There is precisely one topology τ on A such that p is the quotient map. This is the *quotient topology* induced by p.

If we partition a given topological space X and let Y be the set of partitions, then we can construct the *quotient space* by letting p be the surjective map that maps each $x \in X$ to its corresponding partition in Y and letting the topology on Y be induced by p, see [15, p. 139]. Recall in this context the orbit of a group, defined in Section 2.1. The notions of

discreteness, that we will introduce later, allow us to create such a quotient space by mapping each point of a given space onto its orbit under a given group. Later, this will be made more concrete in terms of the discrete groups we consider in this thesis.

Finally, the *genus of a surface* is defined as the maximal number of curves on the surface that, when we cut the surface along these curves, does not disconnect the surface (see [13, p. 163]). We can equivalently think of it as the number of "handles" in the surface. To see this, consider Figure 3.1 and convince yourself that the maximal number of closed curves that does not disconnect the torus is 1. The *genus for a group* is moreover defined as the genus of the quotient surface arising from the group. The latter definition could be given purely algebraically in terms of the structure of generators, which will be touched upon in Section 3.3, together with other phenomena like cusps and cone points.

2.3 Covering Spaces

Of interest in our thesis is also a topological notion that relates the fundamental domains of subgroups to the fundamental domain of the larger group: covering maps and covering spaces. We start with an abstract definition.

Definition 2.7. [14, p. 145] Let X be a path-connected, topological space. An *n-sheeted covering space* (abbreviated as n-sheeted covering), with $1 \leq n \leq +\infty$, for X is a pair $(\tilde{X}, p)$, where $\tilde{X}$ is a topological space and $p : \tilde{X} \to X$ satisfies the following condition: for every point $x \in X$, there is an open neighbourhood $U \ni x$ such that $p^{-1}(U)$ is a disjoint union of n open sets that is each homeomorphically mapped onto U. The map p is called an *n-sheeted covering map* or a *projection*.

As obvious examples, Massey [14, p. 146] gives us that all homeomorphisms $\phi : \tilde{X} \to X$ are 1-sheeted coverings of X. Many, more interesting, examples exist. For instance, quotient surfaces without cone points, discussed later, are covered by the original surface.

There is a problem with restricting ourselves to the covering spaces described, however, since it is often the case in dealing with quotient surfaces, and eminently so in our thesis, that there are exceptional points that give rise to fewer than n sheets in the pre-image, called *branch-points* or *cone points*, [13, p. 207]. Intuitively, this means that when turning a full rotation around the point, only part of a full rotation is actually accomplished. It is probably easier to understand with a picture, see Figure 2.3a. The angle between the two sides at the red point is $2\pi/3$. Thus, when identifying the two sides marked by arrows, making a turn around the red point will only result in a third of a turn.

The displayed domain, in fact, has the hyperbolic plane, in the upper half-plane model, with these exceptional points removed, as a covering space, which can be seen in Figure 5.2.

(a) *Domain pasting around a cone point.*

(b) *The map $z \mapsto z^3$ as an illustration of cone points.*

Figure 2.3: *Visualising cone points.*

A covering space that has such points added is called a *branched covering space*. First of all, we give the general definition, which is:

Definition 2.8. [1, p. 10f] Let X, Y be 2-dimensional spaces. A continuous, surjective map $p : X \to Y$ is a *branched covering map* if there is a discrete subset $S \subset Y$ such that $p : p^{-1}(Y \setminus S) \to Y \setminus S$ is a covering map. Then, X is said to be a *branched* or *ramified* covering space and S the *ramification set*.

In terms of the analytic structure of Riemann surfaces, the equivalent definition is very explicit in how we obtain the branch-points.

Definition 2.9. [13, p. 207] Let $\pi_n : \mathfrak{D} \to \mathfrak{D}$, where $\mathfrak{D}$ is the unit disc, be $\pi_n(z) = z^n$. Then a continuous, surjective map $p : \tilde{S} \to S$ is a *branched covering map* if, for each $s \in S$, there is an open neighbourhood $U \ni s$ such that for each connected component V of $p^{-1}(U)$ there are two homeomorphisms $\Phi : U \to \mathfrak{D}$ and $\Psi : V \to \mathfrak{D}$ with $\Phi \circ p = \Psi \circ \pi_n$ for some n. The corresponding space $\tilde{S}$ is called a *branched* or *ramified* covering space.

Remark 2.3. Consider Figure 2.3b to understand why the map $\pi_n(z) = z^n$ is of relevance in the definition. The 3-sheeted covering of the punctured unit disc $\mathfrak{D} \setminus \{0\}$ comes together at the branch point 0 which is in all sheets, and thus the pre-image $\pi_3^{-1}(0) = \{0\}$ can not satisfy the ordinary demands of a covering surface, but instead must pass via such a map, to give rise to a branched covering. Lifting a path making a full turn around 0 in the unit disc, will only give a third turn in the covering. However, any path entirely in the interior of the surface chart, will not give rise to such behaviour, since they are in the ordinary covering and thus satisfy the 3-to-1-behaviour of such a map.

Applying this definition to the example in Figure 2.3a the reader must, for now, trust that the group that gives rise to this domain also tessellates the entire open upper half-plane, developing this domain by its various

transformations. Thus, we can consider the open upper half-plane as an infinite-sheeted ramified covering space for the domain.

Subgroups will also give rise to covering spaces, as will be seen, when considering an index 6 subgroup of a Fuchsian triangle group in Section 3.4, which gives rise to a 6-sheeted branched covering of the initial group's fundamental domain.

As a preemption of the deep uniformisation theorem, Theorem 3.3, we define a *universal covering space* U of X as a covering space of X that is, moreover, *simply connected*, which means that any path in U can be continuously transformed to a point.

2.4 Hyperbolic Geometry

In order to move to the more mind-bending world of Fuchsian groups, we must first introduce hyperbolic space. The perspective of projective geometry gives us a way to characterise parallel Euclidean lines as those lines that meet at a point at infinity. Thus, the uniqueness of parallel lines corresponds to the "uniqueness of infinity". However, in hyperbolic geometry, there is no such uniqueness. Indeed, given a hyperbolic line l and a point p in the hyperbolic plane not on l, there are infinitely many distinct lines ℓ_i going through p that do not intersect l. And, correspondingly, there is an entire "circle at infinity". In order to distinguish the two different cases, however, not all of them are normally called parallel lines. If ℓ_i meets l in a point on the circle at infinity it is defined as *parallel* and otherwise it is called *ultraparallel*. We mainly follow Beardon [2, p. 126-187], except for his use of the terminology parallel and disjoint in this case.

We will use two models that satisfy the above property, Poincaré's unit disc and upper half-plane models. Several other ways of realising the hyperbolic plane exist, with properties that can be useful in other contexts, but our choice is both a matter of custom and a consequence of the theorems and techniques we are interested in, which are driven towards these models.

Definition 2.10. [2, p. 126f] The *upper half-plane model* of the hyperbolic plane is the set $\mathfrak{U} = \{z : \mathrm{Im}(z) > 0\}$ together with the hyperbolic metric ρ, defined by the differential

$$ds = \frac{|dz|}{\mathrm{Im}\, z}.$$

The *open unit disc model* of the hyperbolic plane is the set $\mathfrak{D} = \{z : |z| < 1\}$ together with the hyperbolic metric ρ^*, defined by the differential

$$ds = \frac{2\,|dz|}{1 - |z|^2}.$$

The *circle at infinity* is defined as $\delta\mathfrak{D} = \{z : |z| = 1\}$ for the disc model and $\delta\mathfrak{U} = \mathbb{R} \cup \{\infty\}$ for the upper half-plane model.

Figure 2.4: *Geodesics in the two models of the hyperbolic plane.*

To calculate the length of a curve in the hyperbolic plane is then a matter of path integration over a parametrisation of the curve with the given differential substituting the Euclidean differential $|dz|$. Let $\gamma(I) \subset \mathfrak{U}$ or $\delta(I) \subset \mathfrak{D}$ be a path of the hyperbolic plane, with the standard notation $z = x + iy$. Then,

$$\rho(\gamma) = \int_\gamma \frac{|dz|}{\operatorname{Im} z} = \int_0^1 \frac{\sqrt{(dx/dt)^2 + (dy/dt)^2}}{y}\, dt,$$
$$\rho^*(\delta) = \int_\delta \frac{2\,|dz|}{1 - |z|^2} \int_0^1 \frac{2\sqrt{(dx/dt)^2 + (dy/dt)^2}}{1 - (x^2 + y^2)}\, dt$$

In order to find the shortest path between two given hyperbolic points z, w, we simply minimise the integral over all the paths between z and w. This path is part of a *geodesic*, which is the equivalent to a Euclidean straight line.[4] The general form of the geodesics has been derived, so that we need not perform the process of minimising $\rho(\gamma)$ in an *ad hoc* fashion. In the "normal" case, the geodesics are Euclidean circles orthogonal to the circle at infinity, in either model. However, in the upper half-plane, when the points have the same real part, we instead get a geodesic that is a vertical Euclidean straight half-line, and in the disc, when the unique Euclidean line through the points contains the origin, the Euclidean line segment inside the unit disc is the hyperbolic geodesic containing the points, explained by Beardon in [2, p. 129-136], see Figure 2.4. Thus, the geodesics are the generalised Euclidean circles orthogonal to the circle at infinity and we will denote the geodesic between α and β as $[\alpha, \beta]$. This characterisation further makes it possible to find the hyperbolic distance efficiently, as in Theorem 2.11.

Theorem 2.11. Let $z, w \in \mathfrak{U}$. The hyperbolic distance $\rho(z, w)$ can be computed by either of the following formulas, used in Appendix A.1:

(i) If $z = iy$, $w = iv$, with $v > y$ then $\rho(z, w) = \ln(v/y)$.

(ii) $\rho(z, w) = \ln\left(|z - \overline{w}| + |z - w|\right) / \left(|z - \overline{w}| - |z - w|\right)$.

[4] For a more physical intuition, consider the geodesics as least energy paths.

Defining the hyperbolic area follows a similar vein as the definition of hyperbolic length. For a set $E \subset \mathfrak{U}$, we define the hyperbolic area as the double integral

$$\mu(E) = \iint_E \frac{dx\ dy}{y^2}.$$

In this case, the non-trivial *Gauss-Bonnet theorem* gives us a way to compute the area of a given polygon with known angles.

Theorem 2.12. [13, Theorem 5.5.2., p. 229] (Gauss-Bonnet) For a hyperbolic triangle Δ with angles $\alpha, \beta, \gamma \geq 0$, $\mu(\Delta) = \pi - \alpha - \beta - \gamma$.

Corollary 2.13. [13, Corollary 5.5.6., p. 230] For a hyperbolic n-gon P, that is hyperbolically convex, with angles $v_1, v_2, \ldots, v_n$,

$$\mu(P) = (n-2)\pi - \sum_{k=1}^{n} v_k$$

Remark 2.4. A set is *hyperbolically convex* if the geodesic line segment between any two points is entirely inside the set, directly translated from Euclidean geometry.

Moving between the two models is achieved by applying the following homeomorphism between the two models that moreover preserves the hyperbolic structure, i.e., it is an isometry between $\mathfrak{U}$ with the metric ρ and $\mathfrak{D}$ with the metric ρ^*, as stated in [2, p. 131] and [20, p. 470].

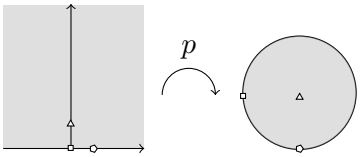

Figure 2.5: *The homeomorphism p between the Poincaré upper half-plane and disc models of hyperbolic geometry.*

Example 2.3. The transformation,

$$p(z) = \frac{z-k}{z-\overline{k}},$$

with $\operatorname{Im} k > 0$, maps the upper half-plane $\{z : \operatorname{Im} z > 0\}$ to the open unit disc $\{z : |z| < 1\}$ bijectively. Thus, its inverse exists and is

$$p^{-1}(z) = \frac{\overline{k}z - k}{z-1}.$$

Since both p and p^{-1} are continuous and defined on the entirety of their respective domain, p is a homeomorphism. The transformation, in the case $k = i$, is illustrated in Figure 2.5 with the mapping of one interior point and two boundary points ($i \mapsto 0$, $0 \mapsto -1$, $1 \mapsto -i$). The transformations, moreover, are *conformal*, i.e., preserves angles, since they are holomorphic maps between the two spaces, see Section 3.1. □

2.5 Möbius Transformations

The final example in Section 2.4 was a particular example of the fundamental building blocks of Fuchsian groups, which are linear fractional transformations. The wealth of material describing and illuminating these Möbius transformations means that we can only give a brief introduction, focused on the scope of our thesis.

Definition 2.14. [13, p. 17] A *Möbius transformation* g is a function of the form

$$g(z) = \frac{az+b}{cz+d},\ ad-bc \neq 0,\ a,b,c,d \in \mathbb{C}.$$

Remark 2.5. This concept can be generalised to higher dimensions by Poincaré's extension method, described extensively in Beardon [2, Ch. 3.3].

The observant reader notices an immediate similarity between this representation of a linear fractional transformation and the matrix group $\mathrm{GL}(2,\mathbb{C})$. Recall that this group is the family of square matrices,

$$\begin{pmatrix} a & b \\ c & d \end{pmatrix},\ ad-bc \neq 0,\ a,b,c,d \in \mathbb{C},$$

defined in [13, p. 18]. One could be tempted to try to define a group isomorphism between these two concepts. However, notice that the Möbius transformation remains invariant when multiplying all elements by some non-zero scalar. This is obviously not true in $\mathrm{GL}(2,\mathbb{C})$, but can be remedied if we construct the quotient group $\mathrm{GL}(2,\mathbb{C})/\{\lambda I : \lambda \neq 0\}$, where we identify all the matrices which differ only by a scalar multiple. Then an isomorphism is accomplished by simply identifying the coefficients in the two groups and this abstract group is called the *projective general linear group* $\mathrm{PGL}(2,\mathbb{C})$ over the field $\mathbb{C}$. When the field is $\mathbb{C}$, we have a special situation, because then $\mathrm{PGL}(2,\mathbb{C})$ is equal to the *projective special linear group* $\mathrm{PSL}(2,\mathbb{C})$, which is instead defined as the *special linear group* of square matrices,

$$\begin{pmatrix} a & b \\ c & d \end{pmatrix},\ ad-bc = 1,\ a,b,c,d \in \mathbb{C},$$

quoted by the set $\{I,-I\}$. This is not true when we want to move to groups over the field $\mathbb{R}$, which Example 2.4 demonstrates.

Example 2.4. Consider the Möbius transformation $g(z) = (3z+4)/(z+2)$, which can be represented in $\mathrm{GL}(2,\mathbb{R})$ as

$$\begin{pmatrix} 3 & 4 \\ 1 & 2 \end{pmatrix}$$

with entries corresponding to the coefficients of g. However,

$$\frac{3z+4}{z+2} = \frac{3\lambda z + 4\lambda}{\lambda z + 2\lambda}$$

for any $\lambda \neq 0$ and thus has infinitely many representatives in $\mathrm{GL}(2,\mathbb{R})$. As can easily be seen, no multiplication with a real $\lambda \neq 0$ will ever yield a negative determinant in the matrix representative, since $\lambda^2 \geq 0$, which implies that the topological group $\mathrm{PGL}(2,\mathbb{R})$ is disconnected, with $\mathrm{PSL}(2,\mathbb{R})$ inside the connected component with pre-images in $\mathrm{GL}(2,\mathbb{R})$ of positive determinant. Since the matrix representatives in $\mathrm{GL}(2,\mathbb{R})$ with determinant precisely 1 are unique, we can identify the Möbius transformations with real coefficients with elements in $\mathrm{PSL}(2,\mathbb{R})$.

Remark 2.6. Since the identification of Möbius transformations with their matrix representatives is so common, we will slightly abuse notation, by letting $g,\ h,\ s,\ t, \ldots$ refer to both the functional representation of an element and the matrix representative of the same element.

As the preceding example states, the group $\mathrm{PSL}(2,\mathbb{R})$ is topological, a fact that is explored in more detail in Section 3.3. With the field of complex numbers, we could move more easily between the general linear form and the special linear form, but as a consequence of the above, we need to be more careful when working with the real numbers. However, we can choose matrix representatives in $\mathrm{PGL}(2,\mathbb{R})$ as long as we stay in the connected component of $\mathrm{PSL}(2,\mathbb{R})$, i.e., we enforce the restriction $ad - bc > 0$. Thus, we define a *real Möbius transformation* as a transformation

$$g(z) = \frac{az+b}{cz+d},\ a,b,c,d \in \mathbb{R},\ ad-bc>0.$$

When moving to Fuchsian groups in Section 3.3, we will use a sequential definition of discreteness, following Beardon [2, p. 11-15] so that a subgroup $G \leq \mathrm{PSL}(2,\mathbb{R})$ is *discrete* if any sequence $\{A_k\}_{k=1}^{\infty} \subseteq G$ such that $a_k, d_k \to 1$, $b_k, c_k \to 0$ as $k \to \infty$ implies that $A_k = I$ for all but finitely many k. There are other equivalent definitions of discreteness, but, in view of the groups we will discuss, this seems the most appropriate.

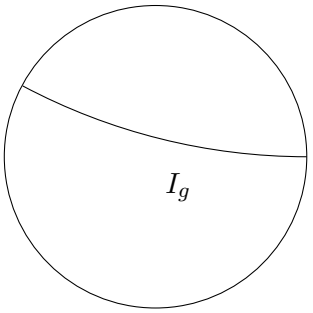

Figure 2.6: *Example of an isometric circle.*

A natural question is why $\mathrm{PSL}(2,\mathbb{R})$ is the natural group to consider in hyperbolic space. This is because this group is one of the crucial descriptors of hyperbolic geometry. Indeed, $\mathrm{PSL}(2,\mathbb{R})$ is the automorphism group of the upper

half-plane model of hyperbolic space, where the *automorphism group*, denoted by $\mathrm{Aut}(X)$, is defined as the group of all conformal homeomorphisms of a given space X. That $\mathrm{PSL}(2,\mathbb{R}) \subset \mathrm{Aut}(\mathfrak{U})$ is a direct result of the following theorem. The other inclusion can be deduced via the theory of analytic functions, see [13, Theorem 4.17.3].

Theorem 2.15. [13, Theorem 5.3.1] For every $g \in \mathrm{PSL}(2,\mathbb{R})$ and every path $\gamma(I) \subset \mathfrak{U}$,

$$\rho(g(\gamma)) = \rho(\gamma).$$

An immediate consequence is, by [13, Theorem 5.3.5], for every pair $z, w \in \mathfrak{U}$,

$$\rho(g(z), g(w)) = \rho(z, w).$$

Finally, one of the important geometric descriptors of a Möbius transformation is the *isometric circle*, and for $g(z) = (az+b)/(cz+d)$ with $c \neq 0$ and $ad - bc = 1$, is defined as the set $I_g = \{z : |cz + d| = 1\}$. In the case $c = 0$, there is no unique circle with the same properties, and then we define, in view of Section 4.3, $I_g = \mathbb{C}$. Moreover, we define the *isometric line* of g as the (Euclidean) perpendicular bisector of the line between the centres of I_g and $I_{g^{-1}}$. An example of an isometric circle in hyperbolic geometry is given in Figure 2.6.

This definition will be amply used in Section 4.1, Section 4.3 and throughout Chapter 5, where the fact that these isometric circles are also hyperbolic geodesics is utilised. However, before going there, we need to delve deeper into the theory of Riemann surfaces and Fuchsian groups.

Chapter 3

Riemann Surfaces and Fuchsian Groups

> ... I left Caen, where I was living, to go on a geologic excursion under the auspices of the School of Mines. The incidents of the travel made me forget my mathematical work. Having reached Coutances, we entered an omnibus to go to some place or other. At the moment when I put my foot on the step, the idea came to me, without anything in my former thoughts seeming to have paved the way for it, that the transformations I had used to define the Fuchsian functions were identical with those of non-Euclidean geometry. I did not verify the idea; I should not have had time, as upon taking my seat in the omnibus, I went on with a conversation already commenced, but I felt a perfect certainty. On my return to Caen, for convenience sake, I verified the result at my leisure. —Henri Poincaré, [16, p. 387f]

3.1 Complex Curves are Real Surfaces

We begin by specifying the characteristics of Riemann surfaces in terms of topology, i.e., building on Section 2.2. The definitions in this section are taken from Jones & Singerman [13, p. 167-172], and we make the natural identification of $\mathbb{C}$ with $\mathbb{R}^2$. We start with an example to tie us back to the previous work.

Example 3.1. [13, p. 2f, 169] In the context of compact Riemann surfaces, one of two special cases is the Riemann sphere. We begin by showing that the Riemann sphere is indeed a surface. First of all, the Riemann sphere is defined as

$$\Sigma = \mathbb{C} \cup \{\infty\},$$

where ∞ is a single point added, such that $z \to \infty$ whenever $|z| \to +\infty$ (distinguishing the point ∞ from the potential infinity $+\infty$). It is then natural to define

$$\frac{1}{0} = \infty, \qquad \frac{1}{\infty} = 0.$$

An atlas $\mathcal{A}$ for Σ consists of two charts, $(\mathbb{C}, z)$ and $(\Sigma \setminus \{0\}, 1/z)$. Thus, Σ is a surface. To show that Σ is a Riemann surface we only need to show that these two charts are analytically compatible. The coordinate transition functions become $z \mapsto 1/z$ on $\mathbb{C} \setminus \{0\}$ in both directions. Clearly this map is analytic on $\mathbb{C} \setminus \{0\}$ and corresponds to rotation around the x-axis in Example 2.2. This means that the charts are indeed analytically compatible.

The abstract definition of a Riemann surface requires us to restrict attention to a certain class of surfaces with a particular structure. It boils down to requiring that we can define analogues of the analytic maps from $\mathbb{C}$ into $\mathbb{C}$, called *holomorphic* maps. Hence, an *analytic atlas* is an atlas with analytic coordinate transition functions. Thus, since the coordinate transition functions in Example 3.1 are both analytic, the Riemann sphere is a Riemann surface. Two analytic atlases are (analytically) *compatible* if $\mathcal{A} \cup \mathcal{B}$ is an analytic atlas. Similarly, one can define other atlases, with other notions of compatibility[1]. Now, compatibility is an equivalence relation, so if there are different equivalence classes of compatible analytic atlases for a given surface, then they will give rise to different structures on the surface, which motivates the definition of a *complex structure* as an equivalence class of analytic atlases. Equivalently, one could define the complex structure as the maximal atlas with respect to analyticity.

All the preceding makes it possible to state what a Riemann surface is in a sentence.

Definition 3.1. A *Riemann surface* is a surface S with a complex structure.

A map $f : S_1 \to S_2$ between two Riemann surfaces S_1 and S_2 is then said to be *holomorphic* if it satisfies the condition that for any pair of charts (U_1, ϕ_1) and (U_2, ϕ_2), respectively for the two surfaces, where $f^{-1}(U_2) \cap U_1 \neq \varnothing$, the induced function $\phi_2 \circ f \circ \phi_1^{-1} : \phi_1(f^{-1}(U_2) \cap U_1) \to \mathbb{C}$ is analytic.

The natural equivalence between Riemann surfaces, corresponding to such notions as homeomorphic in a topological sense, is that of *conformal equivalence*, which means that there is a *holomorphic* homeomorphism between the two surfaces, i.e., preserving both the topological and complex structures on the surface. The conformality of the equivalence is due to the following proposition.

[1] For instance, the compatibility of geometric structures, arising from different metrics on the surface.

Proposition 3.2. [13, p. 198] Let $f : S_1 \to S_2$ be a holomorphic homeomorphism. Then, $f^{-1} : S_2 \to S_1$ is a holomorphic homeomorphism and f and f^{-1} are conformal maps.

Remark 3.1. By using local coordinates, the proof reduces to showing that analytic homeomorphisms are conformal between two open sets $U,\ V \subseteq \mathbb{C}$.

This moves us to a remarkably deep result of Poincaré, Klein and Koebe: all connected Riemann surfaces have one of three universal covering spaces. This is called the *uniformisation theorem*.

Theorem 3.3. [13, Theorem 4.17.2, p. 200] Every simply connected Riemann surface is conformally equivalent to precisely one of:

(i) the Riemann sphere Σ,

(ii) the complex plane $\mathbb{C}$, or

(iii) the hyperbolic plane (in the disc model $\mathfrak{D}$ or the upper half-plane model $\mathfrak{U}$).

Thus, the surfaces are all obtained by making the quotient of the universal covering space with a discrete subgroup of the automorphism group of the universal covering space, see [13, p. 213f], the corresponding groups are so-called fundamental groups for the arising surface. As seen in Example 3.1, the Riemann sphere is of genus 0. In fact, it is the only compact Riemann surface of genus 0 and the only one arising from spherical geometry. The focus of our thesis is on the third possibility, but first we make a detour to quotients of the complex plane.

3.2 The Euclidean Case

The single Riemann surface which arises from Euclidean geometry is the torus, which we now introduce. The material is a synthesis of Beardon [2], Coxeter & Moser [4], Jones & Singerman [13], Voight [20] and Zieschang & al.[22]. The torus arises in a way that is a very good introduction to the way the rest of the compact Riemann surfaces arise in the setting of hyperbolic geometry. First of all, we introduce the lattice Ω over the plane. Together with a fundamental domain, it is displayed in Figure 3.2a. Formally:

Definition 3.4. [13, p. 65f; 20, p. 467] A *lattice* Ω, over two linearly independent basis vectors ω_1 and ω_2 in $\mathbb{C}$ is defined as the set

$$\Omega = \{n\omega_1 + m\omega_2 : n, m \in \mathbb{Z}\}.$$

A *fundamental domain* for Ω is defined to be a closed set D such that

(i) No two distinct points $z, w \in \mathring{D}$ satisfy $z - w \in \Omega$.

(ii) For every point $z \in D^c$ there is either a unique point $w \in \mathring{D}$ such that $z - w \in \Omega$ or two points $w_1, w_2 \in \delta D$, such that $z - w_i \in \Omega$ for $i = 1, 2$.

The lattice is our first example of a discrete group, a notion that will be at the very core of this thesis, so we will try to explain it a bit further.

Recall the definition of a group from Section 2.1. Clearly, the lattice above can be seen as a group, under the translations τ_1 and τ_2 by ω_1 and ω_2. It is additionally a topological group. This can be seen by first considering all the possible translations in the plane as a group operation on $\mathbb{C}$,

$$x \cdot y = m(x, y) : \mathbb{C} \times \mathbb{C} \to \mathbb{C}$$

defined by $m(x, y) = x+y$, with the inverse operation $i(x) = -x$ and identity 0. This is clearly a group operation as well and satisfies the additional criterion of continuity in the topology of $\mathbb{C}$, which defines a *topological group*. Moreover, the lattice Ω considered as a subset of $\mathbb{C}$ is *discrete*, which means that for all $x \in \Omega$ there is a neighbourhood $V \subset \mathbb{C}$, with $x \in V$, such that $V \cap \Omega = \{x\}$. This is indeed the definition of a *discrete group*, a subgroup of a topological group that is also a discrete subset of the topological group. Moreover, in the discrete topology, where all subsets are open, the operations above are continuous on Ω.

Let τ_1 and τ_2 be the translations by ω_1 and ω_2, respectively. Then, the lattice Ω, considered as a group, is generated by τ_1 and τ_2. In this case, there is only one way of combining τ_1 and τ_2 in a non-trivial manner which would yield the identity and that is by commutativity, since ω_1 and ω_2 are linearly independent. In this case we say that a presentation for the group Ω is

$$\langle \tau_1, \tau_2 | \tau_1 \tau_2 \tau_1^{-1} \tau_2^{-1} = e \rangle.$$

Coxeter and Moser [4, p. 1f] describe what generators and relations for a group are in general. The generators for G is a set of elements $\mathcal{E}$ such that every element $g \in G$ can be expressed as some combination of the elements of $\mathcal{E}$ (or their inverses). The defining relations is the set of algebraic equations $\mathcal{R}$ of the form

$$\prod_{k=1}^{n} g_k = e, \ g_k \in G$$

such that every other combination of elements from G that yields the identity can be derived using the rules of algebra and the defining relations. This is called the group's *presentation*, see [22, p. 19], and is denoted $G = \langle \mathcal{E} | \mathcal{R} \rangle$.

Example 3.2. Every cyclic group G_n of finite order n has a presentation of the form $\langle g | g^n = e \rangle$, while an infinite cyclic group has a presentation of the form $\langle g | e \rangle$.

Given all the above we are now ready to construct the compact Riemann surface associated to the lattice Ω. This is done by the topological process of quoting a space by a group. Informally, in this context, we can think of this process as taking out our scissors and cutting out the fundamental domain above and gluing together the sides that correspond to the same vector. For the lattice, then, we need to glue two pairs of sides together, as shown in Figure 3.1. In fact, this is the only way that a compact Riemann surface arises in Euclidean geometry. Recall the definition in Section 2.2 of a

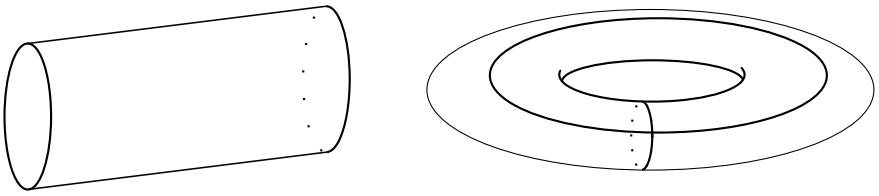

Figure 3.1: *Pasting the fundamental domain for a lattice.*

quotient surface. In terms of discrete groups, we now explain the definition of a *quotient surface*[2] X/G. Let X be a topological space and G a discrete subgroup of the automorphism group of X. Then, X/G is based on the orbits

$$G \cdot x = \{y \in X : y = g \cdot x \text{ for some } g \in G\},$$

which partition X into equivalence classes under the action of G. The quotient surface is then defined as $X/G = \{G \cdot x : x \in X\}$. In terms of the lattice, this identifies the lattice points, in the orbit $\Omega + e$, and for each $x \notin \Omega$, gives rise to an orbit

$$\Omega + x = \{z \in \mathbb{C} : z = n\omega_1 + m\omega_2 + x,\ n, m \in \mathbb{Z}\}.$$

The study of fundamental domains, preferably a polygon, is connected to the quotient spaces, since in the fundamental domain it is only the boundary points that are identified by the quotient. This identification is the pasting that we described informally above and the spaces D/G and X/G coincide as sets. Thus, the problem of the study of group action on an entire space is reduced to the study of the action on the fundamental domain. Working with the identification of sides of a fundamental polygon in the case of a lattice is not necessarily in need of more formalisation, but in view of the material ahead, we introduce the formal definition of how to pair sides for a fundamental polygon D in a geometric space X, as defined in [20, p. 467], but given a slightly different notation. Let S be the set of sides of D. Then, a *side-pairing* for a fundamental polygon D is the set

$$\text{pairs}(D) = \{(g_s, s, s^*) : s \in S,\ g_s(s) = s^*\},$$

[2]Sometimes called the *coset space* $G \setminus X$, to emphasise that we are considering left cosets. Other names are *quotient space*, *quotient set*, *orbit space* & c.

where g_s is an orientation-preserving isometry of X. Two sides s and s^* are said to be *paired* if $(g_s, s, s^*) \in \text{pairs}(D)$ and a vertex v of D is said to be *paired* if the incident sides of v are paired by transformations g_i, $i = 1, 2$, such that $g_i v$ are vertices of D, $i = 1, 2$.

Now, we have not given any justification for choosing the fundamental domain shown in Figure 3.2a. Many other possibilities exist, but there are ways to be more systematic in the way we choose a fundamental domain. There are obvious benefits to this, in terms of added structure, but in the case of the lattice there is also a downside, since the pasting becomes less apparent. The algorithm that we introduce for the lattice produces the Dirichlet domain, since this extends in a natural, albeit not unproblematic, way to the construction of fundamental domains for Fuchsian groups. The

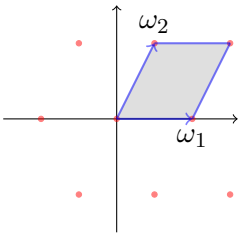

(a) *A fundamental domain for a lattice Ω built from basis vectors.*

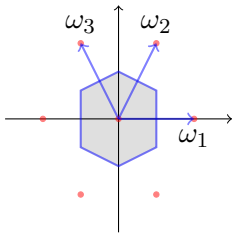

(b) *The Dirichlet fundamental domain for a lattice Ω.*

Figure 3.2: *Fundamental domains for a lattice.*

Dirichlet domain for a lattice Ω[13, p. 68] is defined as the set

$$D(\Omega) = \{z \in \mathbb{C} : |z| \leq |z - \omega|\,, \text{ for all } \omega \in \Omega\}.$$

This means that any point is always at least as close to the origin as it is to any other lattice point. A way to construct the Dirichlet domain in an algorithmic way is to first notice that $0 \in D(\Omega)$ trivially. Then, consider the line segment between 0 and ω, which we will denote by $[0, \omega]$ for all $\omega \in \Omega$. The z that satisfy the defining property with respect to this point lie in the half-plane containing 0 delineated by the perpendicular bisector of $[0, \omega]$. This would seem to be an infinite process, unless one realises that we can restrict attention to the elements

$$\pm\omega_1, \pm\omega_2, \pm\omega_3, \text{ where } \omega_3 = \omega_2 - \omega_1,$$

since the perpendicular bisectors of any other element are at a greater distance from the origin. See Figure 3.2b and Algorithm 3.1.

This presentation is not unique, however, and it is possible to algebraically transform the presentation for a group by *Tietze transformations*, described in Definition 3.5.

Algorithm 3.1 Finding the Dirichlet domain for a lattice Ω.

1. Find the line segments $l_{k,n} = [0, (-1)^n \omega_k]$ for $k = 1, 2, 3$, $n = 0, 1$.
2. Find the perpendicular bisector of $l_{k,n}$ for $k = 1, 2, 3$, $n = 0, 1$.
3. Form the half-plane $H_{k,n}$ bordered by $l_{k,n}$ such that $0 \in H_{k,n}$.
4. Then, $D(\Omega) = \bigcap_{k,n} H_{k,n}$.

Definition 3.5. [22, p. 20f] Let $G = \langle \mathcal{E} | \mathcal{R} \rangle$ be a group with the given presentation. A *Tietze transformation* of G is one of the following

1. Adding a generator g to $\mathcal{E}$, which is derivable from the generators, together with the relation $gw^{-1} = e$, where w is a word in the generators from $\mathcal{E}$.
2. Supposing $g \in \mathcal{E}$ satisfies $g = w$ with w a word in $\mathcal{E} \setminus \{g\}$, the removal of g and the relation $gw^{-1} = e$.
3. Adding relations that are derivable algebraically.
4. Removing relations that are derivable from the others algebraically.

Remark 3.2. The effectiveness of Tietze transformations is that two presentations describe the same group if, and only if, they can be transformed into each other by finitely many Tietze transformations. This theorem is due to Tietze, and is the reason these transformations bear his name. Moreover, we must say that this works in any group, since it is a purely algebraic procedure, and certainly not only in $\mathbb{C}$.

A way to realise such transformations geometrically is to consider domains that represent the different presentations and find how congruent areas can be shifted to correspond to the shift in presentation. Consider Figure 3.3, where the green area has been translated by ω_1, the black area by ω_2 and the red area by $\omega_1 + \omega_2$. In the quotient there is no difference, since congruent points have been exchanged for congruent points. Moving to commutative notation, the Dirichlet domain in this case corresponds to the presentation

$$\langle \tau_1, \tau_2, \tau_3 | \tau_1 + \tau_2 - \tau_1 - \tau_2 = \tau_1 - \tau_2 + \tau_3 = 0 \rangle$$

for the lattice and the fundamental domain derived from the basis vectors corresponds to the presentation

$$\langle \tau_1, \tau_2 | \tau_1 + \tau_2 - \tau_1 - \tau_2 = 0 \rangle$$

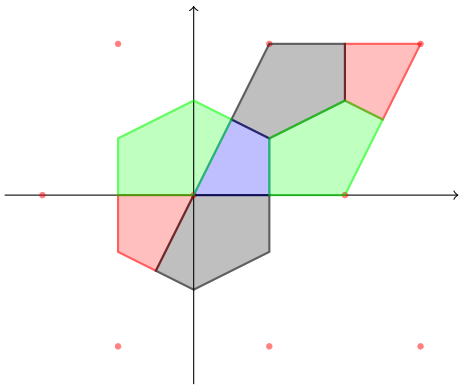

Figure 3.3: *The Dirichlet and basis vector fundamental domains for a lattice with geometric transformations corresponding to Tietze transformations.*

for the lattice. What is represented in Figure 3.3 is the removal of a generator and a relation, by employing the defining relation $\tau_3 = -\tau_1 + \tau_2$. Thus, the generator and the relation for the Dirichlet domain are derivable in the smaller presentation and can be removed safely.

Finally, introducing the torus also gives us a good way to gently acquaint ourselves with another important concept in the study of Riemann surfaces and Fuchsian groups, that of a signature. The first component of the signature is simply the *genus* of the surface D/G, further elucidated in the following section, where we turn to Fuchsian groups which have more complicated structure.

3.3 Fuchsian Groups

With all the preceding in mind, we wish to consider the discrete subgroups of the automorphism group of the hyperbolic plane, called *Fuchsian groups*. They are a direct counterpart of the lattice in Euclidean space, but more difficult to visualise due to their higher-dimensional nature[3]. Fuchsian groups will take on two forms in our thesis, either as subgroups of $\mathrm{PSL}(2,\mathbb{R})$ or of $\mathrm{PSU}(1,1)$. The former has already been introduced as the automorphism group of the upper half-plane model in Section 2.5, whereas the second is the automorphism group of the disc model and can be defined as the group of special unitary matrices quoted by $\{I, -I\}$ or, isomorphically, the group of Möbius transformations

$$g(z) = \frac{az - \overline{b}}{bz + \overline{a}}, \ a, b \in \mathbb{C}, \ a\overline{a} + b\overline{b} = 1,$$

[3]It can be shown that $\mathrm{PSL}(2,\mathbb{R})$ is a 3-dimensional manifold, embeddable in $\mathbb{R}^4$. See [13, p. 231].

see [5, Theorem 23,p. 31]. As is our near-universal custom, we begin with an example.

Example 3.3. All finite subgroups of $\mathrm{PSL}(2,\mathbb{R})$ are obviously discrete. A less trivial, but no less obvious, example is Γ, the *modular group*, which is the subgroup with elements defined by

$$g(z) = \frac{az+b}{cz+d},\ a,b,c,d \in \mathbb{Z},\ ad-bc \neq 0.$$

This group will play an important role in this thesis.

In the same vein as in the Euclidean case, we can construct fundamental domains for Fuchsian groups, that tessellate the hyperbolic plane and give rise to quotient spaces of a much richer nature than the torus. This will give us a natural platform to introduce generalisations of many of the notions presented in Section 3.2. However, in order to give a full picture, we first need to characterise the elements in $\mathrm{PSL}(2,\mathbb{R})$.

We can classify the elements of $\mathrm{PSL}(2,\mathbb{R})$ into three classes[4]. Each class describes properties in the action on the hyperbolic plane, which we will briefly touch on and is defined by the operation $\mathrm{trace}^2(g)$ which is equal to the squared trace of the matrix representative of determinant 1.

Definition 3.6. [2, p. 67] Let g be a Möbius transformation with real coefficients. With the above condition, we define the classification of g according to $\mathrm{trace}^2(g)$:

(i) g is said to be *elliptic* if $0 \leq \mathrm{trace}^2(g) < 4$;

(ii) g is said to be *parabolic* if $\mathrm{trace}^2(g) = 4$;

(iii) g is said to be *hyperbolic* if $\mathrm{trace}^2(g) > 4$.

The way that these transformations act on hyperbolic space is connected to their corresponding isometric circles, defined in Section 2.5. As presented by Ford [5, p. 25-27], the way all the elements of the types above act is first by inversion in the isometric circle followed by reflection in the isometric line. What differentiates them is the relation of the isometric circles I_g and $I_{g^{-1}}$. The way to characterise the classes of elements by isometric circles is to notice that the distance between the centres of the isometric circles I_g and $I_{g^{-1}}$ is $|a/c + d/c|$ and the sum of radii is $2/|c|$, so that we have one of the three possibilities

$$\begin{aligned} &|a/c + d/c| \leq 2/|c|\,, \\ &|a/c + d/c| = 2/|c|\,, \text{ or} \\ &|a/c + d/c| \geq 2/|c|\,, \end{aligned}$$

[4] If we would take $\mathrm{PSL}(2,\mathbb{C})$ instead, there would also exist elements with $\mathrm{trace}^2(g) \notin [0,\infty)$. These are called loxodromic. Some authors join hyperbolic and loxodromic elements into loxodromic elements and call loxodromic elements *strictly* loxodromic.

precisely corresponding to the different classes—since $|a+d| = \sqrt{\text{trace}^2(g)}$. Thus the isometric circle and the inversive isometric circle intersect, are tangent and are exterior to each other precisely when they are elliptic, parabolic and hyperbolic respectively.

Another frequently employed way to characterise the different elements is in terms of their fixed points, see [13, p. 32ff]. Recall that a fixed point of a transformation g is a z such that $g(z) = z$, and thus any iteration of the transformation will keep the point stable. The number and position of fixed points characterises the different transformations. The easiest way to find them in a particular case is simply to solve the quadratic equation

$$cz^2 + (d-a)z - b = 0.$$

With $a, b, c, d \in \mathbb{R}$, and thus working in the upper half-plane model, the only possibilities are two fixed points on the circle at infinity, one fixed point on the circle at infinity of multiplicity 2 or one fixed point inside the hyperbolic plane (the "other" would have to be the complex conjugate, i.e., outside the hyperbolic plane). Simplifying the above equation yields

$$(2cz + (d-a))^2 = (a+d)^2 - 4,$$

which immediately gives the characterisation as one fixed point inside the hyperbolic plane for elliptic transformations, one fixed point on the circle at infinity of multiplicity two for parabolic transformations and two fixed points on the circle at infinity for hyperbolic transformations.

Example 3.4. To give some examples of each type, let

$$g(z) = -\frac{1}{z},\ h(z) = z + 1 \text{ and } s(z) = \frac{z+1}{z+2},$$

where g is elliptic, h parabolic and s hyperbolic, with isometric circles $I_g = \{z : |z| = 1\}$, $I_h = \mathbb{C}$ and $I_s = \{z : |z+2| = 1\}$.

This allows us to extend the notion of a signature for a Fuchsian group based on the structure of the group in terms of its elliptic, parabolic and hyperbolic elements, which we shall now proceed to describe, following [13, p. 219f, 260, 262]. In this, the correspondence between the geometric viewpoint of fundamental domains and the algebraic viewpoint of presentations is very tight and the viewpoints inform each other.

First of all, elliptic elements have one fixed point inside the hyperbolic plane. Thus, for any elliptic transformation, iterating the function will not move the fixed point. Moreover, they are of finite order, by [13, Theorem 5.7.3.]. Thus, every elliptic element of a Fuchsian group is conjugate to an element of the form $z \mapsto e^{2\pi i/n} z$, which is a rotation of the hyperbolic disc. This is demonstrated in Figure 3.4, with an elliptic element of order 2.

The second part of the signature, which we started introducing in Section 3.2, is connected to the elliptic elements. Consider the elliptic element g of order 2 in Figure 3.4. In general, this could be part of a larger finite cyclic group, say of order 4. So, it is not enough to find the elliptic elements, which are of finite order. Instead, the objects of interest are the finite cyclic subgroups of a given Fuchsian group, which are maximal with respect to this property. Moreover, we can conjugate the finite cyclic subgroups, to act with different fixed points. Thus, we need to restrict attention to the conjugacy classes of such maximal subgroups. If we have orders $n_1,\ n_2, \ldots,\ n_k$ for any representatives of the k conjugacy classes, then the signature of G is defined as $\text{sign}(G) = (g; n_1, n_2, \ldots,\ n_k)$.

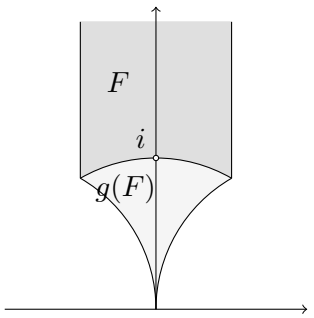

Figure 3.4: *An elliptic element g of order 2, with fixed point i, acting on a region of the hyperbolic plane, by rotation of a half turn.*

Now, recall that a parabolic element has its fixed point on the circle at infinity. If we work in the upper half-plane model, this implies that the fixed point $\alpha \in \mathbb{R} \cup \{\infty\}$. If $\alpha = \infty$, then $c = 0$, so the Fuchsian subgroup that fixes ∞ must be infinite cyclic. Moreover, if $\alpha \in \mathbb{R}$ is the fixed point for $g \in \text{PSL}(2, \mathbb{R})$, then

$$h(z) = \frac{1}{z - \alpha} \in \text{PSL}(2, \mathbb{R})$$

moves α to ∞, so the conjugate $h \circ g \circ h^{-1}$ fixes ∞. Thus, all parabolic subgroups of a given Fuchsian group are infinite cyclic. The action of a parabolic element with fixed point 0 is demonstrated in Figure 3.5a and with fixed point ∞ in Figure 3.5b. As with the elliptic elements, in terms

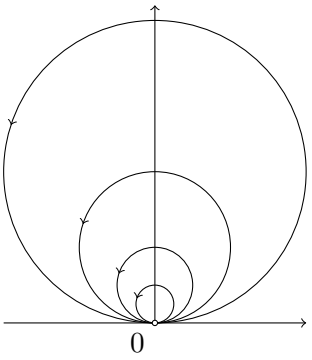

(a) *A parabolic element, with fixed point 0, acting on the hyperbolic plane.*

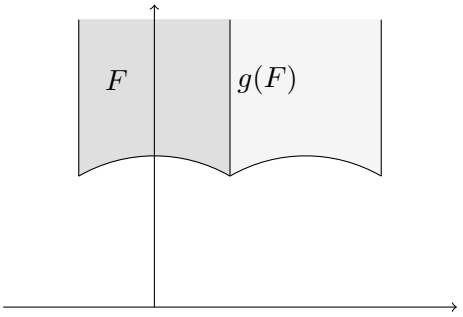

(b) *A parabolic element g, with fixed point ∞, acting on a region of the hyperbolic plane.*

Figure 3.5: *Parabolic elements acting in hyperbolic 2-space.*

of the signature the objects of interest are the conjugacy classes of infinite cyclic subgroups, which are maximal with respect to this property. The different infinite cyclic subgroups are, then, subgroups of the stabilisers of different points on the circle at infinity. The number of such subgroups is the next element in the signature, so the signature of a Fuchsian group with genus g, conjugacy classes of maximal finite cyclic subgroups of orders $n_1, \ldots, n_k$ and s conjugacy classes of maximal infinite cyclic subgroups has signature $(g; n_1, \ldots, n_k; s)$.

Finally, the hyperbolic generators[5] in the group determine the genus of the quotient surface, so that the presentation for the group with signature as above is, by [13, p. 262],

$$\begin{aligned}\langle h_1, t_1, \ldots, h_g, t_g, e_1, \ldots, e_k, p_1, \ldots, p_s | e_1^{n_1} = \cdots = e_k^{n_k} \\ = p_1 \ldots p_s e_1 \ldots e_k h_1 t_1 h_1^{-1} t_1^{-1} \ldots h_g t_g h_g^{-1} t_g^{-1} = e \rangle.\end{aligned}$$

Using the signature of the group it is possible to derive a general formula for the area of its fundamental domain, via the Gauss-Bonnet theorem (Theorem 2.12) and the invariance of the area of a fundamental domain (Theorem 3.8). First we define the Euler characteristic.

Definition 3.7. Let G have signature $(g; n_1, \ldots, n_k; s)$. Then, the *Euler characteristic* is

$$\chi(G) = (2 - 2g) + \sum_{i=1}^{k} (1/n_i - 1) - s.$$

Theorem 3.8. [13, Theorem 5.10.1] For any two fundamental domains F_1, F_2 for a Fuchsian group G, such that δF_1 and δF_2 have vanishing area, the hyperbolic area $\mu(F_1) = \mu(F_2)$.

Theorem 3.9. [13, Theorem 5.10.3, p. 262] Let G have signature $(g; n_1, \ldots, n_k; s)$ and let F be a fundamental domain for G, with $\mu(\delta F) = 0$. Then,

$$\mu(F) = -2\pi\, \chi(G)$$

Example 3.5. The group with signature $(0; 2, 3; 1)$ has fundamental domains with hyperbolic area

$$\mu(F) = 2\pi(-2 + 1/2 + 2/3 + 1) = \pi/3,$$

while the fundamental domains for the group with signature $(0; 3, 3; 1)$ has the hyperbolic area,

$$\mu(F) = 2\pi(-2 + 4/3 + 1) = 2\pi/3.$$

[5] There is another possibility, which we will not discuss here, and that is a fundamental domain with boundary on the circle at infinity, corresponding to hyperbolic boundary elements. This requires much introduction and is not relevant to the groups studied here. A full treatment can instead be found in Beardon [2].

The preceding example, moreover, illustrates a consequence of the fact that there is a Fuchsian group with signature $(0; 2, 3; 1)$ with an index two subgroup of signature $(0; 3, 3; 1)$, because of the following theorem, called the *Riemann-Hurwitz formula*. The explicit computation of this fact is done later, in Section 5.2.

Theorem 3.10. [13, Theorem 5.10.9(ii)] Let G be a Fuchsian group with fundamental domain F and $H \leq G$, with fundamental domain F_n, such that $[G : H] = n < \infty$. If $\mu(F) < \infty$ and $\mu(\delta F) = 0$, then $\mu(F_n) = n\mu(F)$.

This immediately relates the Euler characteristic of a subgroup of finite index to that of the containing group.

Corollary 3.11. Let G be a Fuchsian group with $H \leq G$ and $[G : H] = n < \infty$. Then,

$$\chi(H)/\chi(G) = n.$$

This directly correlates to the topic of our next section, which is the structure of subgroups of Fuchsian groups.

3.4 Fuchsian Subgroups

Our main object in this thesis is to study the modular group and some of its subgroups. To start with, this proposition shows that we do not have to worry in this case about proving discreteness, which, in general, can be a tricky business.

Proposition 3.12. Let G be a Fuchsian group. Then, $H \leq G$ is a Fuchsian group.

Now, given a Fuchsian group of signature $(g; n_1, \ldots, n_k; s)$, there is a way to compute the signatures of the subgroups of a given index n, using a theorem by Singerman[17] on the structure of permutation groups. Using *Reidemeister-Schreier's method*, which will be described shortly, we can then find the explicit generators of this group algorithmically as complex functions, only implicit in the pasting conditions for the N-sheeted covering of the fundamental domain that is produced in Theorem 3.13.

Theorem 3.13. [17, Theorem 1] Let G be a Fuchsian group with signature

$$(g; m_1, \ldots, m_k; s),$$

with e_j, $j = 1, \ldots, k$, the corresponding elliptic elements of order m_j, and p_j, $j = 1, \ldots, s$, the corresponding parabolic elements.

Then, G contains a subgroup G_N, with $[G : G_N] = N$ and signature

$$(g'; n_{11}, \ldots, n_{1\rho_1}, \ldots, n_{k1}, \ldots, n_{k\rho_k}; s')$$

if and only if

(a) There is a finite permutation group P transitive on N points, and an epimorphism $\theta : G \to P$ satisfying:

  (i) The permutation $\theta(e_j)$ has precisely ρ_j cycles of lengths less than m_j, with lengths $m_j/n_{j1}, \ldots, m_j/n_{j\rho_j}$.

  (ii) Denoting the number of cycles in $\theta(\gamma)$ by $\delta(\gamma)$,

$$s' = \sum_{j=1}^{s} \delta(p_j).$$

(b) $\chi(G_N)/\chi(G) = N$.

Proof sketch. We will show part of one direction, in the case of existence of such a permutation group, for elliptic elements. The other direction is short and the parabolic elements are treated very similar to the elliptic elements. This direction of the proof illustrates clearly the use of this theorem later in the thesis, however.

Suppose that P satisfying (i) and (ii) exists. First of all, the stabiliser P_N in P of a point has index N. This implies, by surjectivity, that $G_N := \theta^{-1}(P_N)$ has index N in G. Moreover, any γ in the larger group G permutes the cosets by action on the left. Let γ_i, $i = 1, \ldots, N$ be left coset representatives of G_N. Then, by the epimorphism we induce the same permutation by $\theta(\gamma)$ on the left cosets of P_N represented by $g_i = \theta(\gamma_i)$.

If, for an elliptic element e_j, the image $\theta(e_j)$ has a cycle of length $m_j/n_{j1} = k$, then there are k cosets of P_N cycled by $\theta(e_j)$,

$$\theta(e_j) g_1^{(j)} P_N = g_2^{(j)} P_N, \ldots, e_j g_k^{(j)} P_N = g_1^{(j)} P_N$$

which implies that $g_1^{(j)} P_N = e_j^k g_1^{(j)} P_N$, and also lifts to G and G_N. Thus, for $\gamma = \theta^{-1}(g_1^{(j)})$, the element $\gamma^{-1} e_j^k \gamma$ is in G_N, which then has a period of $m_j/k = n_{j1}$.

In order to show that no two cycles yield the same period of cosets, assume, for contradiction, that $\delta^{-1} e_j^k \delta$ is the element arrived at by the same process above from another cycle and that it is in the same period as $\gamma^{-1} e_j^k \gamma$. Then $\delta^{-1} e_j^k \delta$ is in G_N and is conjugate by $\lambda \in G_N$ to $\gamma^{-1} e_j^k \gamma$, where λ importantly does not permute the cosets since it is in G_N, i.e.,

$$\begin{gathered}
\lambda^{-1}\delta^{-1} e_j^k \delta\lambda = \gamma^{-1} e_j^k \gamma \\
\Longleftrightarrow \\
\lambda^{-1}\delta^{-1}\gamma\gamma^{-1} e_j^k \gamma\gamma^{-1}\delta\lambda = \gamma^{-1} e_j^k \gamma \\
\Longleftrightarrow \\
(\gamma^{-1} e_j^k \gamma)\gamma^{-1}\delta\lambda = \gamma^{-1}\delta\lambda(\gamma^{-1} e_j^k \gamma),
\end{gathered}$$

so $\gamma^{-1}\delta\lambda$ is in the centraliser of $\gamma^{-1}e_j^k\gamma$.[6] Since the centraliser is generated by $\gamma^{-1}e_j\gamma$, $\gamma^{-1}\delta\lambda$ is a power of this element by some p, $1 \leq p \leq m_j$. But then $\delta^{-1}e_j^k\delta$ is in the same period as $\gamma^{-1}e_j^k\gamma$, since

$$\delta G_N = \delta\lambda G_N = \gamma(\gamma^{-1}e_j\gamma)^p G_N = e_j^p\gamma G_N,$$

which is a contradiction. Thus, different k-cycles give rise to different periods.

A very similar argument shows that no cycle gives rise to two periods. □

Example 3.6. We consider as a first example of employing this theorem the triangle group $\Delta(2,4,6)$, which has one order 2 element x_1, corresponding to v_1 in Figure 3.6a with angle π, one order 4 element x_2, corresponding to v_2 with angle sum $\pi/2$, and one order 6 element x_3, corresponding to v_3 with angle $\pi/3$. Now, $x_2 = x_1^{-1}x_3^{-1} = (x_3x_1)^{-1}$, derived from the fact that a counter-clockwise turn around v_2 is first employing x_3 clockwise in the pasting and then x_1 clockwise, i.e., with inverted orientation. This means that we only have two degrees of freedom in choosing the epimorphism. Since there are no parabolic elements, the group is of signature $(0;2,4,6;-)$.

As an aside, all triangle groups are of this form, with $\Delta(l,m,n)$ as $\langle x,y|x^l = y^m = (yx)^n = e\rangle$, and Fuchsian if $1/l + 1/m + 1/n < 1$, see [17, p. 322]. In order to define an appropriate epimorphism it is enough to consider the defining elements

$$\theta(x_1) = (1,4)(2,3)(5,6), \qquad \theta(x_2) = (1,6,5,3)(2,4) \text{ and}$$
$$\theta(x_3) = (1,5,2)(3,4)(6).$$

The epimorphism was found in [12, p. 28]. We can now consider these permutations as pasting conditions. Take 6 copies of the triangle in Figure 3.6a and paste them according to the permutations, as shown in Figure 3.6b. Thus, when pasting the order 2 elements along the cycles of $\theta(x_1)$ we get regular points, the pasting of the order 6 elements along $(1,5,2)$ gives an order 2 element, along $(3,4)$ an order 3 element and along 6 an order 6 element, while the pasting of x_2 is more difficult to see. Consider, however, that 2 and 4 share an order 2 point corresponding to the cycle $(2,4)$ when pasting 1 and 2 and 3 and 4. And that $1,3,5$ and 6 share a regular point in the intersection of the pasting of 6 with 6 and 3 with 4. Finally, the permutations above gives us that the signature is $(g';2,2,3,6;-)$ and with Riemann-Hurwitz's condition we get $g' = 0$.

Theorem 3.13 implicitly gives us the generators of the subgroup. However, in order to get the Dirichlet domain and with a greater correspondence between fundamental domain and generators, we are interested in finding

[6] The subgroup consisting of all elements that commute with the given element.

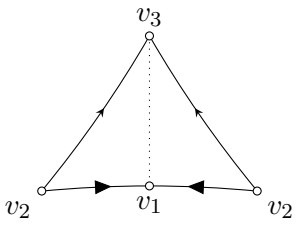

(a) *Pasting of a fundamental domain for the triangle group* $\Delta(2,4,6)$.

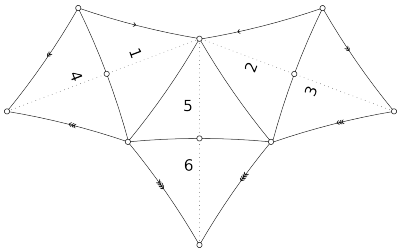

(b) *Pasting conditions for an index* 6 *subgroup of* $\Delta(2,4,6)$.

Figure 3.6: *Fundamental domain for triangle group with subgroup.*

the generators as complex functions. This is in order to be able to apply the algorithm described in Section 4.3 to the subgroups of the modular group which we will study and, moreover, to get a full geometric picture. This can also be done algorithmically, by the method of Reidemeister and Schreier. Here we follow the exposition in [22, Chapter 1]. Since we are only interested in the generators, the details regarding the relations of a subgroup are not discussed and the problem reduces to that of *free groups*, which are abstract groups on a set of symbols, defined as the group with presentation $\langle x_1, x_2, \ldots, x_n | e \rangle$—in the case of a finite presentation— with concatenation of symbols as the group operation, yielding *words* of symbols, such as $x_1 x_2 x_1^{-1} x_2^{-1}$. Recalling Example 3.2, we see that an infinite cyclic group is isomorphic to the free group on one generator—due to a theorem that groups are isomorphic if they have the same presentation [22, Theorem 2.1.2]. The Reidemeister-Schreier method gives us a way to compute the generators of a subgroup as words in the generators of the group.

In order to explain this method, we must define a simple procedure to preserve uniqueness and a correspondence between words of symbols and paths in graphs.

Definition 3.14. Let $\Pi = v_0 e_1^{\pm 1} v_1 e_2^{\pm 1} v_2 e_3^{\pm 1} v_3 \ldots e_n^{\pm 1} v_n$ be a sequence of directed edges e_i, $i = 1, \ldots, n$ and vertices v_j, $j = 0, \ldots, n$ in the directed graph G, such that $e_i^{\pm 1}$ ends in v_i and $e_{i+1}^{\pm 1}$ starts in v_i, for all $i = 1, \ldots, n$, with $+1$ denoting the normal direction and -1 the inverted direction of the traversing of the edge. This will unambiguously be denoted $\Pi = e_1^{\pm 1} e_2^{\pm 1} \ldots e_n^{\pm 1}$. Then Π is said to be a *path* in G, and a *reduced* path is a path such that all occurrences of $e_i e_i^{-1}$, so called *spurs*, have been removed.

Example 3.7. The path $\Pi = e_1 e_2 e_2^{-1} e_1^{-1} e_4$ is not reduced. The corresponding reduced path is $\Pi = e_4$. We can isomorphically consider this as reduction of a word of symbols, with inverses.

Example 3.8. We begin with an example of the Reidemeister-Schreier procedure, which is easily generalised. Consider the graph representing the free

group on two generators G in Figure 3.7a, by letting paths in the graph correspond to concatenations of symbols in the group. An index two subgroup H of G with cosets H and xH gives rise to the graph in Figure 3.7b. A spanning tree B' is marked with a dashed, orange edge. If we base the tree at the vertex e, then this tree is unique, since we want each transition to move us to a node with the entry of the preceding node followed by the edge. Finding the generators is now a matter of selecting edges in $C' \setminus B'$ and finding the unique paths from e to the initial and final vertices of each such edge. In our example we have three edges in $C' \setminus B'$, and one in B'.

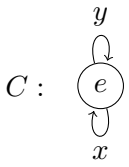

(a) *The Reidemeister-Schreier graph for the free group on two generators.*

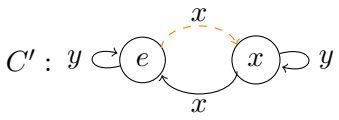

(b) *The Reidemeister-Schreier graph for an index two subgroup of the free group on two generators.*

Figure 3.7: *Examples of Reidemeister-Schreier graphs.*

There is of course some ambiguity in our notation, but we like to keep it close to the word concatenation problem, which will give us the generators. In graph terms what we are doing is first choosing an edge P with initial vertex N in $C' \setminus B'$ and then finding the unique, reduced path from e in B' to the initial vertex (R) and the unique, reduced path from e in B' to the final vertex ($\overline{R}$) of the corresponding edge. Thus, the generators are all the different ways of going out in the graph via B', transitioning via an edge in $C' \setminus B'$ and then moving backwards to e. As a demonstration that it is unnecessary to consider the paths in B', we add the fourth row, since the path is trivially just going out and rolling back the same path.

N	P	R	$\overline{R}$	RP	$\overline{R}^{-1}$	$RP\overline{R}^{-1}$
e	y	e	e	y	e	y
x	x	x	e	x^2	e	x^2
x	y	x	x	xy	x^{-1}	xyx^{-1}
e	x	e	x	x	x^{-1}	e

Table 3.1: *Example of a Reidemeister-Schreier scheme.*

Remark 3.3. It is possible to simply create Table 3.1, without considering the underlying graph, by letting P run through the generators, R through the coset representatives and making all the other computations algebraically. This is how we proceed in this thesis, but the justification for

it is not as easy to see without the complement of combinatorial graphs, however.

The previous extensive example gives the justification for the general method, which is taking this approach and generalising it. The fundamental requirement is the *Schreier condition*, which requires each coset representative to be a word in the generators of the initial group and to have the property that each prefix in the word is a coset representative. This corresponds to the fact that we want to be able to construct B' uniquely with edges moving us to vertices with the vertex label as the previous vertex label concatenated with the edge label. The algorithm is summarised in Algorithm 3.2.

Algorithm 3.2 The Reidemeister-Schreier algorithm for finding generators.

1. Let G be a group with generators $x_1, \ldots, x_k$, $H \leq G$ of index n, and $g_1, \ldots, g_n$ be coset representatives that satisfy the Schreier condition.
2. For each g_i construct a vertex with label g_i and for each generator x_j find the representative for the right coset Hg_ix_j. Draw a directed edge between the corresponding vertices. Denote this graph C'.
3. Construct the spanning tree B' by selecting the unique path from e to the vertices such that the edges in the path are concatenated to the label of the vertex.
4. For each edge f in $C' \setminus B'$, concatenate the unique path in B' from e to its initial vertex with f and the unique counter-directional path in B' from the final vertex of f to e.

Some remarks are due, and the first one is that Reidemeister-Schreier's method is not in any way limited to Fuchsian subgroups, but instead is a general method that works for any group. Moreover, there is a duplication in the table in Example 3.8 above. We do not need both N and R in the table, since the Schreier condition and the construction of the spanning tree guarantees that R will be precisely N. We added this to distinguish the different edges in the graph and to reduce the total amount of notation. Finally, given two complex functions g and h, the symbolic concatenation gh corresponds to the functional composition $g \circ h$.

Now, we are steadily approaching the point where these theorems and algorithms will be employed. The final step before this is to give the theory of fundamental domains for Fuchsian groups in the next chapter.

Chapter 4

Fundamental Domains for Fuchsian Groups

The question of fundamental domains was briefly touched upon in Section 3.2. Here, we will go into some detail of how this translates into the realm of Fuchsian groups.

4.1 Dirichlet and Ford Domains

Now, similar to the treatment on the lattice, we must begin by giving the definition of a fundamental domain for a Fuchsian group. It is instructive to compare this with the definition for a lattice. We say that a closed set D is a *fundamental domain*, [13, p. 240], for the Fuchsian group G if

(i) For each $g \in G$, no two distinct points $z, w \in \mathring{D}$ satisfy $g(z) = w$. This can be equivalently stated as

$$\mathring{D} \cap g(\mathring{D}) = \varnothing$$

for all $g \in G \setminus \{e\}$.

(ii) For every point $z \in D^c$, there is a transformation $g \in G$ such that $g(z) \in D$. This can be equivalently stated as the fact that D tessellates the hyperbolic plane under G, i.e.,

$$\bigcup_{g \in G} g(D) = \mathfrak{U} \text{ or } \mathfrak{D}.$$

Given this definition, there are several ways to construct fundamental domains, just as in the Euclidean case. The two standard domains we will consider are Dirichlet domains and Ford domains. They sometimes overlap as sets, but the ways they are constructed are distinct. Both will be of importance in Section 4.3 and, consequently, throughout Chapter 5.

We discussed the Dirichlet domain for lattices earlier and the notion is similar for Fuchsian groups, at least on an abstract level. The construction of these domains, however, is not at all straight-forward, as was the case for lattices.

The *Dirichlet domain*, [13, p. 241], for a Fuchsian group G centred at p is the set

$$D_p(G) = \{z \in \mathfrak{U} : \rho(z,p) \leq \rho(g(z),p) \text{ for all } g \in G\}. \tag{4.1}$$

As with the Dirichlet domain for lattices, the centre must be in $D_p(G)$ and we could naively approach the problem of obtaining the domain algorithmically by a similar construction, described in Algorithm 4.1. However, the problem here is that we are only guaranteed existence by this approach and not a general method of construction, since the algorithm *a priori* is not even certain to halt. Some ways around this issue will be considered later. Existence

Algorithm 4.1 Naively finding the Dirichlet domain for a Fuchsian group G.

1. Choose a centre $p \in \mathfrak{U}$.
2. Find the (hyperbolic) line segments $l_g = [p, g(p)]$ for $g \in G$.
3. Find the (hyperbolic) perpendicular bisector of l_g for $g \in G$.
4. Form the (hyperbolic) half-plane H_g bordered by l_g such that $p \in H_g$.
5. Then, $D(G) = \bigcap_{g \in G} H_g$.

of a Dirichlet domain is, then, due to the fact that $\rho(z,p) \leq \rho(g(z),p)$ precisely describes the half-plane H_g for g and taking the intersection over all members, yields the Dirichlet domain, by definition. First of all, the Dirichlet domain does not map interior points to interior points, trivially, by noticing that the interior of the domain is described by the inequalities $\rho(z,p) < \rho(g(z),p)$. Moreover, the hyperbolic plane is tessellated by the Dirichlet domain under the elements, due to the discreteness of G implying the existence of an element with smallest hyperbolic distance to p, in every G-orbit over $\mathfrak{U}$, which thus must be in the Dirichlet domain. (See [13, Theorems 3.1.3, 3.4.5,p. 241].)

In the special case of a finite group, however, we can employ the above method directly.

Example 4.1. Two of the smallest Fuchsian groups are the cyclic groups generated by $-1/z$ and $-1/(z+1)$, of order 2 and 3 respectively. Their respective fundamental domains are presented in this example as illustration of the naive approach.

(i) We first consider the finite group consisting of the elements $e(z) = z$ and $g_1(z) = -1/z$. We first choose the centre of the Dirichlet domain as $p = 2i$. Then, $g_1(2i) = i/2$, so that the hyperbolic perpendicular bisector of the line segment $[i/2, 2i]$ is the upper half of the unit circle, since the point of intersection between the imaginary axis and the bisector is iy, $y > 0$, where $\rho(i/2, iy) = \rho(2i, iy)$ is fulfilled. This is equivalent, by Theorem 2.11, to the equation

$$\ln(y/(1/2)) = \ln(2/y).$$

Moreover, the perpendicularity condition forces the centre of the circle to be the origin. Thus, the fundamental domain for the group is displayed in Figure 4.1a. The reader should however not be deceived by the Euclidean intuition that the area in the interior of the displayed circle is finite. Every fundamental domain for a Fuchsian group has the same invariant area (assuming that the boundary has vanishing area), see Theorem 3.8, which in this case is infinite.

(ii) For the group consisting of $e(z) = z$, $g_1(z) = -1/(z+1)$ and $g_2(z) = -(z+1)/z$, we once again choose $p = 2i$ as our centre. In Figure 4.1b, the geodesics connecting the images of $2i$ under g_1 and g_2 are drawn in blue and the perpendicular bisectors in black.

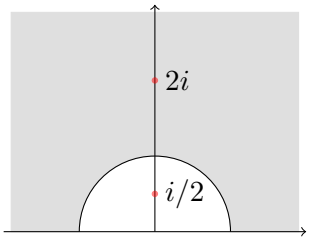

(a) *Fundamental domain for a cyclic Fuchsian group of order* 2.

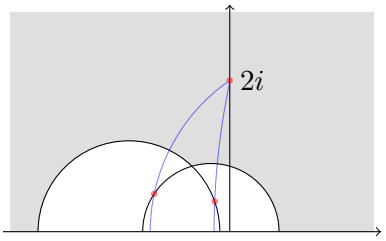

(b) *Fundamental domain for a cyclic Fuchsian group of order* 3.

Figure 4.1: *Fundamental domains for finite Fuchsian groups.*

A more interesting case is the modular group, Γ, which is generated by both of the two elements $-1/z$ and $-1/(z+1)$, given in Example 4.1.

Example 4.2. [13, p. 242-244] The Dirichlet domain centred at ki, $k > 1$, for Γ is the intersection of the hyperbolic half-planes given by the perpendicular bisectors of $[ki, ki+1]$, $[ki, ki-1]$ and $[ki, i/k]$, i.e., bounded by the vertical lines $\mathrm{Re}(z) = -1/2$, $\mathrm{Re}(z) = 1/2$ and the segment between these lines of the unit circle, seen in Figure 4.2. This immediately implies that the Dirichlet domain for Γ centred at ki is a subset of this set. The other inclusion is shown by the reflective symmetry of the Dirichlet domain centred at ki around the imaginary axis, i.e., $z \in D_{ki}(\Gamma)$ implies $-\overline{z} \in D_{ki}(\Gamma)$.

Define the reflection $r(z) = r^{-1}(z) = -\overline{z}$, which is an isometry. For any $g \in \Gamma$, $r \circ g \circ r^{-1} \in \Gamma$ and by the invariance of the hyperbolic metric under isometries,

$$\rho(r(z), ki) = \rho(z, ki) \leq \rho(r^{-1}(g(r(z))), ki) = \rho(g(r(z)), ki),$$

so $-\overline{z}$ must also be part of $D_{ki}(\Gamma)$. The next step in the process is to show that if a transformation of Γ takes a point z of F to another point w of F, then both z and w must be boundary points and either has z as a fixed point or takes z to its mirror image in the imaginary axis, $w = -\overline{z}$. By combining this with the above, the result will be fairly immediate. We begin with the conclusion however, since this will give the motivation for taking this step. Assume that $g \in \Gamma$ takes $z \in F$ to $w \in F$, then by the following, they will both be on the boundary of F and either

$$w = z \Longrightarrow \rho(z, ki) = \rho(g(z), ki),$$

or

$$w = -\overline{z} \Longrightarrow \rho(z, ki) \leq \rho(g(z), ki),$$

by the above. This will thus establish the inclusion. Now, let

$$g(z) = \frac{az + b}{cz + d},\ ad - bc = 1,\ \text{with } a, b, c, d \in \mathbb{Z},$$

such that $g \neq e$ and consider the points z and $w = g(z)$, both in F. First of all, we want to establish that the imaginary parts of z, w are the same. Since $w \in F$,

$$|cz + d|^2 = c^2 |z|^2 + 2cd \operatorname{Re}(z) + d^2 \geq c^2 - cd + d^2 = (c - d)^2 + cd \geq 1,$$

using the penultimate expression when $cd \leq 0$ and the final expression when $cd > 0$, to establish the inequality. This immediately implies that $\operatorname{Im}(w) \leq \operatorname{Im}(z)$ and by exchanging for g its inverse, we obtain the equality of imaginary parts and, since

$$\operatorname{Im}(w) = \operatorname{Im}(z) / |cz + d|^2$$

also the equality $|cz + d|^2 = 1$. Then we also obtain the enclosure

$$0 \leq cd \leq 1,$$

by considering the two equalities that follow, together with the integrality of c, d:

$$(c - d)^2 = 1 - cd$$
$$(c + d)^2 = 1 + 3cd.$$

This gives us three possibilities.

(1) $c = 0, ad = 1$. Then, $a = d = \pm 1$ and b can take any integer value. These are the transformations $z \mapsto z + n$ for $n \in \mathbb{Z}$. But, the only possibility for $g(z)$ to be in F is that $n = \pm 1$ and then z and w must be mirror images in the imaginary axis and found on the geodesics $\mathrm{Re}(z) = \pm 1/2$.

(2) $d = 0, bc = -1$. Then $b = -c = \pm 1$ and a can take any integer value. This gives rise to the family of transformations

$$a - \frac{1}{z}$$

but for this to send z into F, $a = 0, \pm 1$, since all points in the interior of F are inverted into the unit disk and then translated by a. In the case $a = \pm 1$, $z = w$ and they are one of the vertices, i.e., the intersection between the geodesics $\mathrm{Re}(z) = \pm 1/2$ and the unit circle. If $a = 0$, then $w = -\overline{z}$ by simple algebra and lies on the unit circle, the only part of F that remains invariant under the transformation.

(3) $cd = 1$, i.e., $c = d = \pm 1$. Now, we can expand the identity obtained previously

$$|cz + d|^2 = c^2 |z|^2 + 2cd\,\mathrm{Re}(z) + d^2 = 1,$$

which in this case gives us $(|z|^2 - 1) + (2\,\mathrm{Re}(z) + 1) = 0$ which implies $|z| = 1$ and $\mathrm{Re}(z) = -1/2$, so z must be $-1/2 + i\sqrt{3}/2$. Then, the fact that the imaginary parts are equal and that g transforms z into a point in F implies that $g(z)$ must be $\pm 1/2 + i\sqrt{3}/2$.

This finishes the argument that the domain in question is indeed the Dirichlet domain centred at ki, and more generally, a fundamental domain.

Now, Example 4.1 is illustrative as a starting point of how we approach the Dirichlet domain in hyperbolic space, but not very enlightening in how we could approach groups in general. In order to lay the ground work for the algorithmic approach later described and implemented, we need to consider another way to construct fundamental domains, based on the isometric circles defined in Section 2.5. This is the Ford domain.

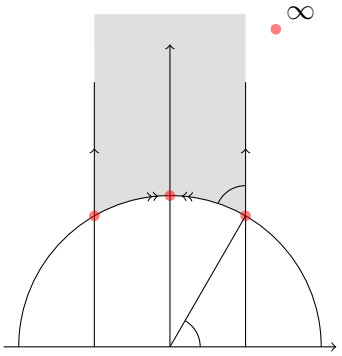

Figure 4.2: *The Dirichlet domain centred at ki for* Γ *in the upper half-plane model, with vertices marked as red dots and congruent sides marked with arrows.*

Definition 4.1. Let g be a Möbius transformation with coefficients $a, b, c, d \in \mathbb{C}$, $ad - bc = 1$. If $c \neq 0$, the *exterior domain of* g is $\mathrm{ext}(g) = \{z : |cz + d| > 1\}$. If $c = 0$, we define $\mathrm{ext}(g) = \mathbb{C}$.

Let $G \leq \mathrm{PSU}(1,1) = p\,\mathrm{PSL}(2,\mathbb{R})\,p^{-1}$, be a set of Möbius transformations acting on $\mathfrak{D}$, with p one of the homeomorphisms described in Example 2.3. Then, the *exterior domain of* G is

$$\mathrm{ext}(G) = \overline{\overline{\bigcap_{g \in G} \mathrm{ext}(g) \cap \mathfrak{D}}}.$$

If G, moreover, is a Fuchsian group acting on the hyperbolic disc, then the exterior domain, as defined here, is called the *Ford domain for* G.

That the Ford domain is a fundamental domain is established by Ford in [5, p. 44-46, 67]. The method is more general than for Fuchsian groups and considers all groups that work on the extended complex plane Σ. The extra property of Fuchsian groups is that the common fixed circle, also called the *principal circle* by Ford, of all such groups is the boundary of a model of the hyperbolic plane, which corresponds to the fact that they are subgroups of the automorphism group of the hyperbolic plane. Furthermore, [5, Theorem 1, p. 67] gives us that the isometric circles of a Fuchsian group are orthogonal to the boundary of the hyperbolic plane, i.e., they are geodesics. This implies that if we consider the isometric circles and $\delta\mathfrak{D}$ as subsets of Σ, then inversion in $\delta\mathfrak{D}$ will carry the Ford domain, as a domain in Σ, into itself and the interiors of isometric circles into themselves. Thus, all results are valid if we only consider the hyperbolic disc model, and by homeomorphism, the upper half-plane model.

We proceed in the more general manner, considering the domain without the intersection with $\mathfrak{D}$. Briefly, transformations map the exterior of their isometric circle into the interior of the isometric circle of the inverse transformation, which means that condition (i) for a fundamental domain is fulfilled. Showing that any point in the hyperbolic plane is congruent to a point of the Ford domain is a lengthier process, involving a proof by contradiction, which we will only sketch. First consider a circle C with no points of the Ford domain nor points congruent to it, centred at $z_0 \in \mathbb{C}$. Then, z_0 is either in the interior or on the boundary of an isometric circle I_g of a transformation g, which by extension must be true of the entire orbit of z_0 under the group in question. Since all transformations map the centres of their isometric circles to ∞, which is in the domain, the orbit of z_0 can not contain any such centres. Using some knowledge of the action of elements in relation to their isometric circles, briefly touched upon in Section 3.3, an iterative scheme arises that generates a transformation of C of arbitrarily large radius, which is a contradiction of the assumption that C contained no congruent points, since the radii of isometric circles are bounded from above, by [5, p. 41]. Thus, the Ford domain also satisfies the second requirement of fundamental domains, by the general method and by the remarks on how to restrict ourselves to Fuchsian groups.

Remark 4.1. Using the disc model is potentially much easier conceptually than the upper half-plane model when considering Ford domains, since we do not have the point ∞ to consider, but can work with only circles and need not consider generalised circles. Including groups with a fixed point at ∞ takes extra care, and a further exposition of this is detailed in [5, p. 75-78].

The final theorem that connects the two domains and makes the algorithm which we present in Section 4.3 effective is the following.

Theorem 4.2. [20, p. 471] Let $G \leq \mathrm{PSU}(1,1)$ be a Fuchsian group acting on $\mathfrak{D}$. Then, $D_0(G) = \mathrm{ext}(G)$.

4.2 Sides and Vertices on Fundamental Polygons

One of the reasons that fundamental polygons are so interesting is the close correspondence of the characteristics of the polygon and how the group acts on its vertices and sides on the one hand and the algebraic presentation on the other. In this section, we will describe this connection further by presenting and illustrating Poincaré's side-pairing theorem. Recall from Section 3.2 the definition of a side-pairing, i.e., two sides s and s^* of a polygon are paired by an element $g \in G$ if $g(s) = s^*$. If we have a pairing of all the sides in a polygon, all the vertices are also paired by these elements. The following is a summary of [13, p. 245-247, 255]

Example 4.3. Consider the fundamental domain for Γ in Figure 4.2. The vertical sides are paired by $g(z) = z + 1$ and the circle segment is paired to itself by $h(z) = -1/z$. The vertices are, moreover, fixed by different elements. The ideal vertex ∞ is fixed by g, while the vertex i is fixed by h and the vertices $-1/2+i\sqrt{3}/2$ and $1/2+i\sqrt{3}/2$ are fixed by $s(z) = -1/(z+1)$ and $g \circ s \circ g^{-1}(z) = (z-1)/z$.

The preceding example gives us occasion to discuss several general patterns that are demonstrated there. First of all, we define an *elliptic vertex* as a vertex that is fixed by an elliptic element. In the side-pairing it will be part of a cycle of vertices that are all elliptic, since if g maps s to s^* and $v_1 \in s$ is fixed by the elliptic element e_1, then $g(v_1) \in s^*$ is fixed by the elliptic element $g \circ e_1 \circ g^{-1}$. The angle sum of such a cycle corresponds to the order of the group generated by any element fixing one of the vertices: there is a conjugacy class of maximal finite cyclic subgroups of order n if, and only if, there is a corresponding cycle of elliptic vertices with angle sum $2\pi/n$, see [2, Theorem 9.3.5].

Moreover, the ideal vertex ∞ is fixed by g. Since g is a parabolic element, ∞ is called a *parabolic vertex*. The angle at such a vertex is defined as 0.

Finally, there is a point which we called a vertex in Example 4.3 which is not a vertex in the normal sense. The reason is that it is the fixed point

of an order two elliptic element, namely $-1/z$. Such elements pair sides to themselves and their fixed point is *on* the side. One can thus consider the fixed point as a vertex and the side as two sides, or alternatively, allow self-pairings.

In the above, we have gone from the group to the geometry. The theorem of Poincaré also reverses this process, so that under certain natural conditions, one moves backwards to receive a group by its generators and relations from a given polygon and pairings. This means that there is a two-way correspondence between algebra and geometry.

Theorem 4.3. [2, Theorem 9.8.4] Let P be a hyperbolic polygon with side-pairing pairs(P) and let G be the group generated by the pairing elements g_s in pairs(P). If,

(i) for each vertex v of P, there are vertices $v_0,\ v_1, \ldots, v_n$ of P and elements $f_0, \ldots, f_n$ of G which constitute a cyclic pairing of sides, i.e., $f_{j+1} = g_s \circ f_j$, with $v_0 = v$ and $f_0 = f_{n+1} = e$, and

$$f_j\left(\{y \in \overline{P} : \rho(y, v_j) < \varepsilon\}\right)$$

are non-overlapping and forms the union $B(v, \varepsilon)$.

(ii) ε can be chosen independently of v in $\overline{P}$,

then G is a Fuchsian group and P is a fundamental polygon for P.

Remark 4.2. This somewhat technical theorem can in many cases be rephrased as a set of side and angle sum conditions, see [19, p. 170, 180].

Example 4.4. The fundamental domain $D_{ki}(\Gamma)$ for Γ has side-pairing elements $g(z) = z + 1$ and $h(z) = -1/z$. By Poincaré's theorem the group generated by g and h is Fuchsian and has P for fundamental domain. This group is, naturally, Γ.

4.3 Algorithmic Computation of Fundamental Domains

Since the problem of finding the Dirichlet domain in general is non-trivial, as seen in Example 4.2, it is interesting to note that in certain cases, using some special structures it is possible to calculate it explicitly using an algorithmic approach. One such approach is the one studied by John Voight in [20]. This algorithm is based on certain assumptions, that in general, can be difficult to determine, but in specific and interesting cases are known to hold. His main theorem is, in a somewhat simplified form,

Theorem 4.4. Let G be a Fuchsian group generated by a known finite set, whose members have coefficients in an algebraic field extension of $\mathbb{Q}$ and suppose that G is a cofinite group, i.e., its fundamental domain has finite area. Moreover, let $p \in \mathfrak{U}$ not be fixed by any element in $G \setminus \{I\}$. Then, there is an algorithm which returns the Dirichlet domain $D_G(p)$, a side-pairing of $D_G(p)$ and a minimal finite presentation for G.

This approach is useful for instance in the case of a large class of Fuchsian groups called *arithmetic*, which are known to be cofinite, but which we will not go into here. But, as will be apparent later, when we study the modular group and its subgroups, this method is useful in this case as well.

Remark 4.3. If we have a group like the modular group, which acts on $\mathfrak{U}$, we need to conjugate it first to act on $\mathfrak{D}$, in order for the algorithms in this chapter to work. See Section 3.3.

We need a few new concepts to systematically find Dirichlet domains, but we begin with a birds-eye view of the process.

1. If $H \subset G$ is finite, then we can compute a normalised boundary of
$$E = \text{ext}(H).$$
2. Given a finite subset $H \subset G$, we can reduce every element $\gamma \in G$ with respect to H.
3. Using the known relation $\langle H \rangle = G$, we can find a normalised basis for G, by reduction.

Now, the above summary introduces many undefined concepts, which we will now begin to unravel. First of all, the normalisation concepts are clearly intertwined.

Definition 4.5. A *normalised basis* H for a group G is a generating set for G, such that $\text{ext}(H)$ is a fundamental domain for G, and that forms a normalised boundary for $\text{ext}(H)$. Now, a *normalised boundary* for a domain $D = \text{ext}(H)$ is a sequence
$$U = (g_1, g_2, \ldots, g_n)$$
such that (i) $D = \text{ext}(U)$; (ii) $I_{g_1}, \ldots, I_{g_n}$ contain the counterclockwise consecutive sides of D; (iii) the vertex $v \in D$ with minimal argument $\arg(v) \in (0, 2\pi)$, where v is considered as a complex number, is either a proper vertex of the meet of I_{g_1} and I_{g_2} or an ideal vertex with $v \in I_{g_1}$.

This is enough to take care of the first step in the process. The input is $H \subseteq G$ finite. The output is a normalised boundary U of $\text{ext}(H)$ in $\mathfrak{D}$. We make sure we find the vertices in cyclic order so that the argument of the vertex in each subsequent step is minimised. This will yield a sequence that satisfies the above definition.

Algorithm 4.2 Finding a normalised boundary for $\mathrm{ext}(H)$.

1. Initialise $\theta := 0$, $U := \varnothing$ and $L := [0, 1]$.
2. Let B be the set of $g \in H$ such that $\arg(I_g \cap L) \geq \theta$.

   If $B = \varnothing$, choose $g \in H$ that minimises the argument of the initial vertex of I_g in $[\theta, \theta + 2\pi)$.

   Else, choose $g \in B$ that minimises the argument of the meet of I_g and L in $[\theta, \theta + 2\pi)$, such that the meeting angle is minimal.
3. If $g \in U$, return the normalised boundary U.

   Else update U by appending g, $L := I_g \cap \overline{\mathfrak{D}}$, θ to the minimal argument found in 2. Go to step 2.

Example 4.5. Finding the normalised boundary for an exterior domain is exemplified in Figure 4.3, where the boundary is taken counter-clockwise from the point 1 in the complex plane.

The second step is the reduction process, which is the core process that allows us to reduce the problem of computing a fundamental domain to an algorithm in finite time. Recall the naive approach given in Algorithm 4.1, which, in comparison, is *not* guaranteed to end in finite time. This requires an introduction of the map

$$\mathrm{r} : G \to \mathbb{R}^+,$$

which is defined for groups acting on $\mathfrak{D}$ by

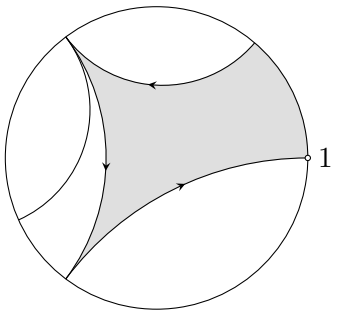

Figure 4.3: *Example of a normalised boundary.*

$$\gamma \mapsto \mathrm{r}(\gamma; z) = \rho^*(\gamma(z), 0).$$

We then say that an element $\gamma \in G$ is (H, z)-*reduced* if, for a fixed $z \in \mathfrak{D}$ and for all $g \in H$, $\mathrm{r}(g \circ \gamma; z) \leq \mathrm{r}(\gamma; z)$ and H-*reduced* if $z = 0$.

The reduction algorithm in Algorithm 4.3 takes as input an ordered set $H \subset G \setminus \{I\}$, $\gamma \in G$, and $z \in \mathfrak{D}$ and returns two group elements, $\mathrm{red}_H(\gamma; z) \in G$ and $\delta \in \langle H \rangle$, such that $\mathrm{red}_H(\gamma; z)$ is (H, z)-reduced and $\mathrm{red}_H(\gamma; z) = \delta \circ \gamma$. If $z = 0$, we abbreviate $\mathrm{red}_H(\gamma; 0) = \mathrm{red}_H(\gamma)$. Reducing γ in this way is a straight-forward iteration, where halting is ensured by the discreteness of G.

Algorithm 4.3 Computing $\mathrm{red}_H(\gamma; z) = \delta \circ \gamma$.

1. Initialise $\hat{\gamma} := \gamma$ and $\delta := e$.

2. Compute $r := \mathrm{r}(\hat{\gamma}; z)$ and for each $g_i \in H$, compute $r_i := \mathrm{r}(g_i\hat{\gamma}; z)$ and, then, compute $\underline{r} := \min_i r_i$.

   If $r \leq \underline{r}$, then return $\mathrm{red}_H(\gamma; z) = \hat{\gamma}$ and δ.

   Else let $\underline{g} := g_i$ be such that $r_i = \underline{r}$ and for any $r_j = \underline{r}$, $i \leq j$.

3. Update $\hat{\gamma} := \underline{g} \circ \hat{\gamma}$ and $\delta := \underline{g} \circ \delta$. Go to step 2.

Example 4.6. Let H be the set of transformations

$$g_1(z) = \frac{(1+i/2)z - i/2}{iz/2 + 1 - i/2}, \qquad g_1^{-1}(z) = \frac{(1-i/2)z + i/2}{-iz/2 + 1 + i/2},$$
$$g_2(z) = \frac{(1-2i)z - 2i}{2iz + 1 + 2i}, \qquad g_2^{-1}(z) = \frac{(1+2i)z + 2i}{-2iz + 1 - 2i},$$

then the reduction algorithm above, which is easily verified, yields that the reduction $\mathrm{red}_{H\setminus\{g_1\}}(g_1; 0) = e(z)$, with $\delta(z) = g_1^{-1}(z)$. This corresponds to the fact that g_1 is in any group with g_1^{-1} as a generator.

This makes it possible to construct a normalised basis for $\langle H \rangle$, and thus if we know a finite generating set for G, we can construct a normalised basis for G. Algorithm 4.4 is, in essence, a matter of finding a normalised boundary for the exterior domain of the generators and their inverses, and then successively adding elements to use for the exterior domain until the domain has a side-pairing. There is a slight clarification in Step 5 compared with the article. This clarification has been made in private correspondence with the article author.

For computational purposes, we employed `C++` together with the `GiNaC` library, see [7]. Common functionality is found in Appendix A.1, the implementation of Algorithm 4.3 in Appendix A.2 and finding approximate pairings for step 5 of Algorithm 4.4 in Appendix A.3. Since the `GiNaC` library does not support symbolic square roots out of the box, any plausible pairings were double-checked with `Wolfram|Alpha`, see [21].

One of the main objectives of this thesis is using this algorithm for subgroups of a particular Fuchsian group, which was introduced earlier, the modular group. In order to start our investigation, we will turn to the modular group, Γ, and compute a fundamental domain for this group.

Algorithm 4.4 Computing a normalised basis for $\langle H \rangle$.

As input we take an ordered set $H = (g_1, \ldots, g_t)$. Let $H^{-1} := (g_1^{-1}, \ldots, g_t^{-1})$.

1. Update $H := H \cup H^{-1}$.

2. Compute the normalised boundary U of $\mathrm{ext}(H)$ by Algorithm 4.2.

3. Let $H' := U$. For each $g \in H$, compute $\hat{g} = \mathrm{red}_{H\setminus\{g\}}(g)$ using Algorithm 4.3. If $\hat{g} \neq e$, update $H' := H' \cup \{\hat{g}\}$.

4. Compute the normalised boundary U' of $\mathrm{ext}(H')$.

   - If $U' = U$, then set $H := H'$. Go to step 5.
   - Else set $U := U'$. Go to step 3.

5. Let $E := \mathrm{ext}(U)$ and let V be the set of vertices of E not paired by elements in H.

   - If $V = \varnothing$, then return the normalised boundary U.
   - Else, for each $g_k \in H$, such that $v_k \in V \cap I_{g_k}$, compute

   $$\hat{g}_k := \mathrm{red}_H(g_k; v_k), \quad k = 1, \ldots, m.$$

   For ideal vertices, the reduction is instead made on a point in I_{g_k} that is hyperbolically closer to $I_{g_k^{-1}} \setminus E$.

   Update $H := H \cup \bigcup_{k=1}^{n} \hat{g}_k$ and go to step 2.

Chapter 5

Computations for Specific Fuchsian Groups

Turning to concrete computations, we will consider the modular group Γ, its only index 2 subgroup, its two index 3 subgroups and another type of subgroup, which is of index 6.

5.1 The Modular Group Γ

The first concrete group that we shall consider in more depth is the modular group, which, the reader will recall, is the subgroup of $\mathrm{PSL}(2,\mathbb{R})$ which has the further constraint that its coefficients are limited to the integers. Thus, it is denoted $\mathrm{PSL}(2,\mathbb{Z})$, but more briefly Γ, and can be defined as the set of Möbius transformations,

$$g(z) = \frac{az+b}{cz+d},\ a,\ b,\ c,\ d \in \mathbb{Z},\ ad-bc \neq 0.$$

As a consequence of Example 4.4, this group is generated by the functions,

$$s(z) = z+1 \text{ and } \ t(z) = -1/z.$$

Using the knowledge of these generators, we can compute the fundamental domain algorithmically.

The first step is to conjugate the two generators s and t to act on $\mathfrak{D}$ instead of $\mathfrak{U}$. In order to do this, we must first choose an appropriate homeomorphism, so that our choice of centre is mapped onto 0 of $\mathfrak{D}$, since the algorithm generates a Dirichlet domain with centre 0 of the disc model. In order for the algorithm to work, we need to have a trivial stabiliser of the centre. Now, take $g \in \Gamma$. Then, for $k > 1$,

$$g(ki) = \frac{aki+b}{cki+d} = \frac{bd+ack^2+ki}{c^2k^2+d^2} = ki$$

is equivalent to the system of equations, together with the requirement on the determinant,

$$\begin{cases} bd + ack^2 = 0 \\ c^2k^2 + d^2 = 1 \\ ad - bc = 1 \end{cases}$$

If $c = 0$, then $b = 0, d = \pm 1, a = d$, so $g(z) = z$. If $c \neq 0$, however, $c^2k^2 > c^2 \geq 1$, since $k > 1$, so no such element can satisfy the second equation. Thus, ki is not fixed by any non-trivial element of Γ.

Choose $k = 2$ and conjugate the matrix representatives of s and t as follows.

$$g_1 := p \circ s \circ p^{-1} = \begin{pmatrix} 1 & -2i \\ 1 & 2i \end{pmatrix} \begin{pmatrix} 1 & 1 \\ 0 & 1 \end{pmatrix} \begin{pmatrix} 1/2 & 1/2 \\ i/4 & -i/4 \end{pmatrix} = \begin{pmatrix} 1 + i/4 & -i/4 \\ i/4 & 1 - i/4 \end{pmatrix},$$
$$g_2 := p \circ t \circ p^{-1} = \begin{pmatrix} 1 & -2i \\ 1 & 2i \end{pmatrix} \begin{pmatrix} 0 & -1 \\ 1 & 0 \end{pmatrix} \begin{pmatrix} 1/2 & 1/2 \\ i/4 & -i/4 \end{pmatrix} = \begin{pmatrix} -5i/4 & -3i/4 \\ 3i/4 & 5i/4 \end{pmatrix}.$$

It is trivial to show that such a conjugation indeed gives generators for the conjugate group. Per Algorithm 4.4, we let $H := (g_1, g_2, g_1^{-1}, g_2^{-1})$, where $g_1^{-1} = \overline{g_1}$ and $g_2^{-1} = -g_2$. Next, we must compute the normalised boundary of $\text{ext}(H)$ and this requires us to compute the isometric circles of the elements of H. The reader is encouraged to follow the process by simultaneously viewing Figure 5.1. The isometric circles are

$$I_{g_1} = \{z : |z - 1 - 4i| = 4\}, \qquad I_{g_2} = \{z : |z + 5/3| = 4/3\},$$
$$I_{g_1^{-1}} = \{z : |z - 1 + 4i| = 4\}, \qquad I_{g_2^{-1}} = I_{g_2}.$$

The final equality is due to the fact that $g_2 = g_2^{-1}$ as transformations, and by projective identification of the matrix representatives. As stated in Algorithm 4.2 we initialise $\theta := 0$, $U := \varnothing$ and $L := [0, 1]$.

1. The only isometric circle that intersects L with argument greater than or equal to 0 is I_{g_1}, so we update $U := (g_1)$, $L := I_{g_1} \cap \overline{\mathfrak{D}}$ and $\theta := 0$.

2. The only isometric circle that intersects L with argument greater than or equal to 0 is I_{g_2}, so we update $U := (g_1, g_2)$, $L := I_{g_2} \cap \overline{\mathfrak{D}}$ and $\theta \approx 2.5536$.

3. The only isometric circle that intersects L with argument greater than or equal to θ is $I_{g_1^{-1}}$, so we update $U := (g_1, g_2, g_1^{-1})$, $L := I_{g_1^{-1}} \cap \overline{\mathfrak{D}}$ and $\theta \approx 3.7296$.

4. Finally, we would get I_{g_1} again. But, then we are done and the algorithm returns the normalised boundary (g_1, g_2, g_1^{-1}).

Then, we let $H' := (g_1, g_2, g_1^{-1})$. We compute the reductions

$$\hat{g}_1 = e, \qquad \delta_1 = g_1^{-1}, \qquad \hat{g}_2 = e, \qquad \delta_2 = g_2^{-1}$$
$$\hat{g}_1^{-1} = e, \qquad \delta_1^{-1} = g_1, \qquad \hat{g}_2^{-1} = e, \qquad \delta_2^{-1} = g_2.$$

Since all reductions are the identity, there is nothing to add to H' and trivially the normalised boundary of $\mathrm{ext}(H')$ is U. Thus, we update H to (g_1, g_2, g_1^{-1}). The vertices of $\mathrm{ext}(U)$ are $v_1 = 1$, $v_2 = (6\sqrt{3} - 15 - i(4\sqrt{3} - 10))/13$ and $v_3 = \overline{v_2}$. Now,

$$g_1(v_1) = g_1^{-1}(v_1) = v_1,\ g_1(v_2) = v_3 \text{ and } g_1^{-1}(v_3) = v_2,$$

so all sides are paired and there is no need for further iterations. Since all Möbius transformations are conformal, the mapping of the three vertices under p^{-1} is enough to establish the domain in the upper half-plane,

$$p^{-1}(v_1) = \infty,\ p^{-1}(v_2) = \frac{-1 + i\sqrt{3}}{2} \text{ and } p^{-1}(v_3) = \frac{1 + i\sqrt{3}}{2},$$

which is familiar, since this is precisely the domain displayed in Figure 4.2.

5.2 The Index Two Subgroup of Γ

Our next object of investigation is the first of the subgroups of the modular group: the one of index two, i.e., that splits the modular group in two cosets. We will show that there is only one such group, by employing the theorem described in Section 3.4. The problem of finding all such subgroups reduces to constructing the possible epimorphisms $\theta : \Gamma \to C_2$, where C_2 is the cyclic permutation group on two elements.

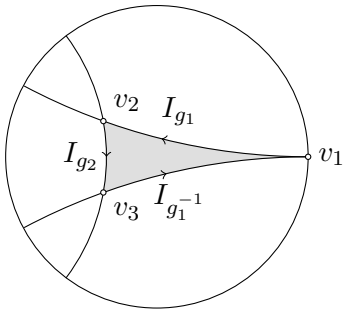

Figure 5.1: *The isometric circles of g_1, g_2 and g_1^{-1} and their exterior domain with normalised boundary for Γ.*

Given the presentation of Γ, which is $\langle x, y | x^2 = y^3 = e \rangle$, there are only two possibilities that determine the epimorphism entirely. The first possibility is $\theta(x) = (1, 2)$ and $\theta(y) = (1)(2)$, where thus $\theta(xy) = (1, 2)$. Now, the signature of Γ is $(0; 2, 3; 1)$. Then, by applying Theorem 3.13, $\theta(x)$ has 1 cycle of length $2 \leq 2$ for x, 2 cycles of length $1 \leq 3$ for y and for the parabolic element xy one cycle of length 2. The only stabiliser of points in this group is the trivial one. So $\theta^{-1}(\{(1)(2)\}) = \ker(\theta)$ has the signature $(g'; 3, 3; 1)$. From now on, we will use the simplifying notation $G_2 := \ker(\theta)$. From the relation $[G : H] = \chi(H)/\chi(G)$ for $H \leq G$, we get

$$\chi(G_2) = 2g' - 2 + \frac{2}{3} + \frac{2}{3} + 1 = 2 \cdot \chi(\Gamma) = \frac{1}{3},$$

so $g' = 0$. Thus, the signature of this group is $\text{sign}(G_2) = (0; 3, 3; 1)$.

If we follow Jones & Singerman [13] in the Tietze transformation of the presentation, and the corresponding fundamental domain in Figure 4.2, whereby the part of the domain with $-1/2 \leq \operatorname{Re} z \leq 0$ is moved to $1/2 \leq \operatorname{Re} z \leq 1$, a geometric view of the subgroup in hyperbolic space is easier to see. The order 2 element corresponding to the vertex at i has been eliminated, and thus a turn around the point in the quotient space is a full circular rotation, and the point is thus regular, indicated by green points. However, the order 3 elements have been duplicated, thus yielding the cone points, indicated by red points.

If we try to use the other possible epimorphism, with $\theta(x) = (1)(2)$ and $\theta(y) = (1, 2)$, it does not satisfy the cycle conditions, since we need the orders of the group m_j to be divisible by the cycle lengths c_k,

$$m_j/n_{j,k} = c_k \Longleftrightarrow m_j/c_k = n_{j,k}.$$

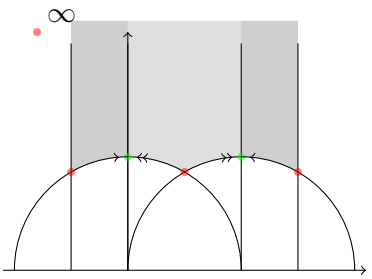

Figure 5.2: *A fundamental domain for the index two subgroup of* Γ*, constructed by the implicit pasting conditions of the construction from Singerman's theorem.*

Further, in order to algorithmically produce a fundamental domain we need to find the generators of the subgroup, by applying the Reidemeister-Schreier method. This requires us to consider the group Γ abstractly as a set of words in the symbols x and y with the presentation above, which we recall is $\langle x, y | x^2 = y^3 = e \rangle$. As previously stated in Section 3.4 we only need to consider the free group on the generators of Γ in order to find the generators of the subgroup, i.e., the group $S = \langle x, y | e \rangle$.

Now, consider Table 5.1, where we let R run through the right coset representatives of G_2 and P through the generators of Γ, by Remark 3.3.

R	P	$\overline{R}$	RP	$\overline{R}^{-1}$	$RP\overline{R}^{-1}$
e	x	x	x	x^{-1}	e
e	y	e	y	e	y
x	x	e	x^2	e	e
x	y	x	xy	x^{-1}	xyx^{-1}

Table 5.1: *Reidemeister-Schreier scheme for* $G_2 \leq \Gamma$.

According to the Reidemeister-Schreier method, the final column is then a listing of the generators of G_2, which is thus generated by the two elements,

$$s(z) = -\frac{1}{z+1}, \qquad t(z) = \frac{z-1}{z}.$$

The observant reader will spot that $t(s(z)) = z + 2$, which should be expected from the domain shown previously in Figure 5.2 and which gives the

alternative generators s and ts. Since $G_2 \leq \Gamma$, we already know that $p = 2i$ is fixed by no element of G_2, so no problem arises if we use this point as our centre for the Dirichlet domain. Thus, we conjugate the matrices, as in Section 4.3,

$$\begin{aligned} g_1 := p \circ s \circ p^{-1} &= \begin{pmatrix} 1 & -2i \\ 1 & 2i \end{pmatrix} \begin{pmatrix} 0 & -1 \\ 1 & 1 \end{pmatrix} \begin{pmatrix} 1/2 & 1/2 \\ i/4 & -i/4 \end{pmatrix} \\ &= \begin{pmatrix} 1/2 - 5i/4 & -1/2 - 3i/4 \\ -1/2 + 3i/4 & 1/2 + 5i/4 \end{pmatrix}, \\ g_2 := p \circ t \circ p^{-1} &= \begin{pmatrix} 1 & -2i \\ 1 & 2i \end{pmatrix} \begin{pmatrix} 1 & -1 \\ 1 & 0 \end{pmatrix} \begin{pmatrix} 1/2 & 1/2 \\ i/4 & -i/4 \end{pmatrix} \\ &= \begin{pmatrix} 1/2 - 5i/4 & 1/2 - 3i/4 \\ 1/2 + 3i/4 & 1/2 + 5i/4 \end{pmatrix}. \end{aligned}$$

We let $H := (g_1, g_2, g_1^{-1}, g_2^{-1})$, where

$$g_1^{-1} = \begin{pmatrix} 1/2 + 5i/4 & 1/2 + 3i/4 \\ 1/2 - 3i/4 & 1/2 - 5i/4 \end{pmatrix} \text{ and } g_2^{-1} = \begin{pmatrix} 1/2 + 5i/4 & -1/2 + 3i/4 \\ -1/2 - 3i/4 & 1/2 - 5i/4 \end{pmatrix}.$$

Thus, the isometric circles are

$$\begin{aligned} I_{g_1} &= \{z : |z + 11/13 - 16i/13| = \frac{4}{\sqrt{13}}\}, \\ I_{g_2} &= \{z : |z + 19/13 + 4i/13| = \frac{4}{\sqrt{13}}\}, \\ I_{g_1^{-1}} &= \{z : |z + 19/13 - 4i/13| = \frac{4}{\sqrt{13}}\}, \\ I_{g_2^{-1}} &= \{z : |z + 11/13 + 16i/13| = \frac{4}{\sqrt{13}}\}. \end{aligned}$$

To give a good walk-through of a concrete example we will be very detailed in this section, at least for the first encounter with a problem. In the following sections we will presume that the reader will be able to fill in the details. Step 1 is then to set $H := (g_1, g_2, g_1^{-1}, g_2^{-1})$. Step 2 is to find a normalised boundary U of $\text{ext}(H)$.

1. $\theta := 0$, $U := \varnothing$, $L := [0, 1]$. Then, $B = \varnothing$ and v_2 is the vertex with minimal argument. Since $g_1 \notin U$, we continue.

2. $\theta :\approx 76.5396°$, $U := (g_1)$, $L := I_{g_1} \cap \mathfrak{D}$. Then, $B = \{x_1\}$, with g_1^{-1} unique candidate. Since $g_1^{-1} \notin U$, we continue.

3. $\theta :\approx 146.31°$, $U := (g_1,\ g_1^{-1})$, $L := I_{g_1^{-1}} \cap \mathfrak{D}$. Then, $B = \{x_2\}$, with g_2 unique candidate. Since $g_2 \notin U$, we continue.

4. $\theta := 180°$, $U := (g_1,\ g_1^{-1},\ g_2,)$, $L := I_{g_2} \cap \mathfrak{D}$. Then, $B = \{x_3\}$, with g_2^{-1} unique candidate. Since $g_2^{-1} \notin U$, we continue.

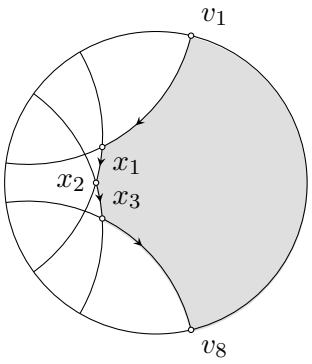

(a) *The isometric circles of* g_1, g_2, g_1^{-1} *and* g_2^{-1} *and their exterior domain with normalised boundary.*

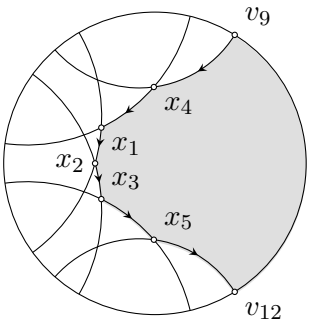

(b) *The isometric circles of* g_1, g_2, g_1^{-1}, g_2^{-1}, g_3 *and* g_4 *and their exterior domain with normalised boundary.*

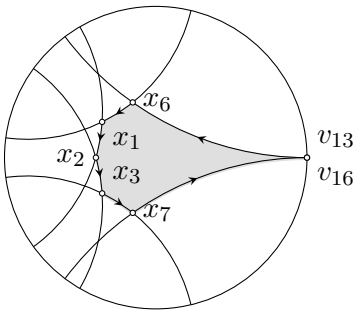

(c) *The isometric circles of* g_1, g_2, g_1^{-1}, g_2^{-1}, g_5 *and* g_5^{-1} *and their exterior domain with normalised boundary.*

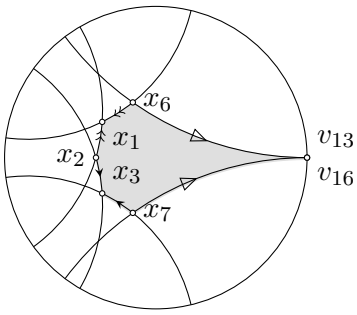

(d) *The isometric circles of* g_1, g_2, g_1^{-1}, g_2^{-1}, g_5 *and* g_5^{-1} *and their exterior domain, with side-pairing.*

Figure 5.3: *Algorithmic computation for* G_2*, all figures.*

5. $\theta :\approx 283.4604°$, $U := (g_1, g_1^{-1}, g_2, g_2^{-1})$, $L := I_{g_2^{-1}} \cap \mathfrak{D}$. Then, $B = \varnothing$ and the minimal argument vertex is v_2. Since $g_1 \in U$, we return U as the normalised boundary, displayed in Figure 5.3a.

We set $H' := U$ and since the reductions in Table 5.2a are all the identity, there is nothing to add to H' and since $H' = U$, the exterior domain $\text{ext}(H') = \text{ext}(U)$, so we move to Step 5. To see which vertices are paired we compute $g_i(v_j)$ for all $g_i \in H$ and all $v_j \in V$, where V is the set of vertices of $\text{ext}(U)$. In Table 5.2b, we see that x_1 and x_3 are paired, so we update $V := \{v_1,\ x_2,\ v_8\}$. Then, we perform the reductions on the

g	$\text{red}_{H\setminus\{g\}}(g)$
g_1	e
g_1^{-1}	e
g_2	e
g_2^{-1}	e

(a) *G_2: Reductions of elements in step 3, iteration 1.*

g	v	$g(v)$	g	v	$g(v)$
g_1	v_1	$\notin V$	g_1^{-1}	v_1	$\notin V$
	x_1	x_1		x_1	x_1
	x_2	$\notin V$		x_2	$\notin V$
	x_3	$\notin V$		x_3	$\notin V$
	v_8	$\notin V$		v_8	$\notin V$
g_2	v_1	$\notin V$	g_2^{-1}	v_1	$\notin V$
	x_1	$\notin V$		x_1	$\notin V$
	x_2	$\notin V$		x_2	$\notin V$
	x_3	x_3		x_3	x_3
	v_8	$\notin V$		v_8	$\notin V$

(b) *G_2: Pairing of vertices in step 5.*

Table 5.2: *G_2: reductions and pairing.*

unpaired vertices. In Table 5.3, we display the numerical values for the unpaired vertices and in Table 5.4 we display the reductions and associated information. Throughout this thesis, the ideal vertices are approximated by the intersection of the isometric circle and the circle $|z| = \sqrt{97/100}$.

v	v_{num}
v_1	$\frac{1}{75400}\left(112\sqrt{164671} - 28171 + i(40976 + 77\sqrt{164671})\right)$
x_2	$\frac{1}{13}\left(8\sqrt{3} - 19\right)$
v_8	$\overline{v_1}$

Table 5.3: *G_2: Unpaired vertices in step 5.*

Thus, we get the new elements g_3 and g_4, which we add to G, while we do not add $\pm g_1^{-1}$, since they are both the same element projectively and are thus already in the set.

We return to step 2. The normalised boundary is now instead

$$U := (g_3, g_1, g_1^{-1}, g_2, g_2^{-1}, g_4),$$

g	v	$\mathrm{red}_H(g; v_{num})$	δ
g_1	v_1	$g_3 := \begin{pmatrix} 3/2-3i/4 & -1/2-5i/4 \\ -1/2+5i/4 & 3/2+3i/4 \end{pmatrix}$	g_2^{-1}
g_1	x_2	$-g_1^{-1} = \begin{pmatrix} -1/2-5i/4 & -1/2-3i/4 \\ -1/2+3i/4 & -1/2+5i/4 \end{pmatrix}$	g_1
g_1^{-1}	x_2	$g_1^{-1} = \begin{pmatrix} 1/2+5i/4 & 1/2+3i/4 \\ 1/2-3i/4 & 1/2-5i/4 \end{pmatrix}$	e
g_2^{-1}	v_8	$g_4 := \begin{pmatrix} 3/2+3i/4 & -1/2+5i/4 \\ -1/2-5i/4 & 3/2-3i/4 \end{pmatrix}$	g_1

Table 5.4: *G_2: Reductions on vertices in step 5.*

displayed in Figure 5.3b. We go to step 3 and perform the reductions (the previous ones are obviously valid still and will not yield anything new), displayed in Table 5.5. Thus, $H' := (g_3, g_1, g_1^{-1}, g_2, g_2^{-1}, g_4, g_5, g_5^{-1})$, whose exterior domain is $U' = (g_5, g_1, g_1^{-1}, g_2, g_2^{-1}, g_5^{-1})$, displayed in Figure 5.3c. Thus, we update $U := U'$ and go to step 3, which trivially yield the same reductions, but nothing gets added to H', so $U' = U$ in step 4 and we proceed to pairing vertices with $H := H'$ in step 5. The pairing is then, $g_1([x_6, x_1]) = [x_2, x_1]$, $g_2([x_2, x_3]) = [x_7, x_3]$ and $g_5([x_6, v_{13}]) = [x_7, v_{16}]$. The algorithm then returns the exterior domain as a fundamental domain with a side-pairing, displayed in Figure 5.3d.

g	$\mathrm{red}_{H\setminus\{g\}}(g)$	g	$\mathrm{red}_{H\setminus\{g\}}(g)$
g_3	$g_5 := \begin{pmatrix} 1+i/2 & -i/2 \\ i/2 & 1-i/2 \end{pmatrix}$	g_4	g_5^{-1}

Table 5.5: *G_2: Reductions of elements in step 3, iteration 2.*

5.3 The First Index Three Subgroup of Γ

As was demonstrated in Section 5.2, the cycle conditions of Singerman's theorem impose restrictions on the epimorphisms that we can construct to induce subgroups of the modular group. When dealing with index three subgroups, we will only consider epimorphisms that yield valid cycle conditions.

Our first example of an index three subgroup is the one which is induced by the epimorphism, $\theta : \Gamma \to \Sigma_3$, where Σ_3 is the full symmetry group on three points, defined by

$$\theta(x) = (1,2)(3),\ \theta(y) = (1,2,3) \text{ and } \theta(xy) = (1)(2,3).$$

Let $X = \mathrm{Stab}_{\Sigma_3}(3) = \{e, (1,2)\}$. Then, X has index three in Σ_3 and we let $G_{3,1} := \theta^{-1}(X)$ be the corresponding index three subgroup of Γ. By

Singerman's theorem, $\text{sign}(G_{3,1}) = (g'; 2; 2)$. Riemann-Hurwitz' formula then gives us

$$\chi(G_{3,1}) = 2g' - 2 + 1/2 + 2 = 3 \cdot \chi(\Gamma) = 1/2 \iff g' = 0.$$

Further, the right coset representatives of $G_{3,1}$ are chosen as $e,\ y$ and y^2,

R	P	RP	$\overline{R}$	$\overline{R}^{-1}$	$RP\overline{R}^{-1}$
e	x	x	e	e	x
e	y	y	y	y^{-1}	e
y	x	yx	y^2	y	yxy
y	y	y^2	y^2	y	e
y^2	x	y^2x	y	y^{-1}	y^2xy^2
y^2	y	e	e	e	e

Table 5.6: *Reidemeister-Schreier scheme for* $G_{3,1} \leq \Gamma$.

corresponding to $\theta(e) = e,\ \theta(y) = (1,2,3)$ and $\theta(y^2) = (1,3,2)$. Thus the Reidemeister-Schreier scheme goes according to Table 5.6. Since $y^2xy^2 = (yxy)^{-1}$, we can skip one of these generators and we choose x and yxy as our generators. Thus, we have the generators of $G_{3,1}$ as Möbius transformations,

$$s(z) = -\frac{1}{z}, \qquad t(z) = -\frac{1}{z+2}.$$

This, similarly to the index two subgroup, gives rise to the element $z \mapsto z + 2$. We proceed to compute the fundamental domain of $G_{3,1}$. Thus, the generators, as acting on $\mathfrak{D}$, are

$$g_1 := p \circ s \circ p^{-1} = \begin{pmatrix} -5i/4 & -3i/4 \\ 3i/4 & 5i/4 \end{pmatrix}$$
$$g_2 := p \circ t \circ p^{-1} = \begin{pmatrix} 1 - 5i/4 & -1 - 3i/4 \\ -1 + 3i/4 & 1 + 5i/4 \end{pmatrix}$$

First, the initial exterior domain is displayed in Figure 5.4a and the reductions in step 3 are displayed in Table 5.7. Since g_1 pairs I_{g_1} to itself, but no

g	$\text{red}_{H\setminus\{g\}}(g)$
g_1	$g_3 := \begin{pmatrix} 1 - i/2 & i/2 \\ -i/2 & 1 + i/2 \end{pmatrix}$
g_2	e
g_2^{-1}	e

Table 5.7: $G_{3,1}$*: Reductions of elements in step* 3*, iteration* 1.

other side is paired, the set of unpaired vertices of the exterior domain in Figure 5.4b is $V = \{v_3,\ v_4,\ v_7,\ v_8\}$, displayed with their approximations in

v	v_{num}
v_3	$\frac{1}{8200}(197+32\sqrt{24823}+i(6304-\sqrt{24823}))$
v_4	$\frac{1}{8200}(197-32\sqrt{24823}+i(6304+\sqrt{24823}))$
v_7	$\frac{1}{1000}(197-2\sqrt{155191}+i(-394-\sqrt{155191}))$
v_8	$\frac{1}{1000}(197+2\sqrt{155191}+i(-394+\sqrt{155191}))$

Table 5.8: *$G_{3,1}$: Unpaired vertices for iteration 1, step 5.*

g	v	$\mathrm{red}_H(g; v_{num})$	δ
g_2	v_3	$g_4 := \begin{pmatrix} -1+13i/4 & 3-5i/4 \\ 3+5i/4 & -1-13i/4 \end{pmatrix}$	$\begin{pmatrix} -3-3i/2 & -2-5i/2 \\ -2+5i/2 & -3+3i/2 \end{pmatrix}$
g_2	v_4	$g_3^{-1} := \begin{pmatrix} -1-i/2 & i/2 \\ -i/2 & -1+i/2 \end{pmatrix}$	g_1
g_3	v_7	g_3	e
g_3	v_8	g_3	e

Table 5.9: *$G_{3,1}$: Reductions on vertices in step 5.*

Table 5.8. The reductions on the unpaired vertices are displayed in Table 5.9. Since this yields the side-pairing $g_1([v_1, v_2]) = [v_2, v_1]$, $g_3([v_7, v_8]) = [v_{10}, v_9]$ we are done. The final domain is displayed with normalised boundary in Figure 5.4c and with side-pairing in Figure 5.4d.

5.4 The Second Index Three Subgroup of Γ

Our second, and final, example of index three[1] is the group, denoted $G_{3,2}$, induced by the epimorphism

$$\theta(x) = (1)(2)(3),\ \theta(y) = (1,2,3) \text{ and } \theta(xy) = (1,2,3),$$

which yields the signature $(0; 2, 2, 2; 1)$. The coset system for this group is chosen as e, y and y^2. The Reidemeister-Schreier scheme is then displayed in Table 5.10, where in the last column we employ the relations of Γ. The generators are then, as complex functions,

$$h_1(z) = -1/z,\ h_2(z) = -\frac{z+1}{2z+1} \text{ and } h_3(z) = -\frac{z+2}{z+1}$$

where h_1 corresponds to x, h_2 to yxy^{-1} and h_3 to $y^{-1}xy$.

Since $x = x^{-1}$, another set of generators is

$$s_1(z) = -1/z,\ s_2(z) = \frac{z-2}{z-1} \text{ and } s_3(z) = \frac{z+1}{z+2},$$

[1] One more epimorphism satisfies the cycle conditions, but does not satisfy the Riemann-Hurwitz identity, instead yielding genus -1, which is clearly impossible.

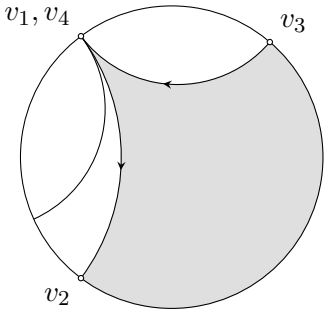

(a) *The isometric circles of* g_1, g_2 *and* g_2^{-1} *and their exterior domain with normalised boundary.*

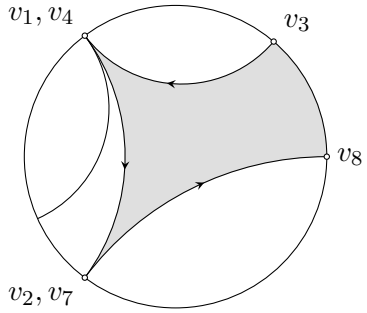

(b) *The isometric circles of* g_1, g_2, g_2^{-1} *and* g_3 *and their exterior domain with normalised boundary.*

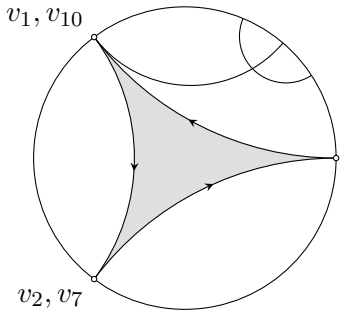

(c) *The isometric circles of* g_1, g_2, g_3, g_3^{-1} *and* g_4 *and their exterior domain with normalised boundary.*

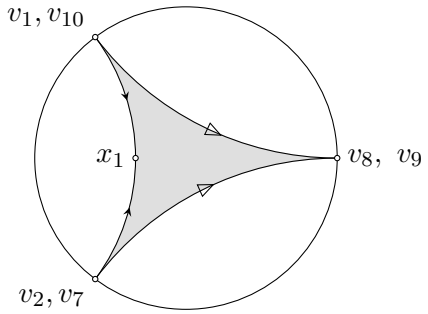

(d) *The isometric circles of* g_1, g_3, *and* g_3^{-1} *with fundamental domain and side-pairing.*

Figure 5.4: *Algorithmic computation for* $G_{3,1}$*, all figures.*

R	P	RP	$\overline{R}$	$\overline{R}^{-1}$	$RP\overline{R}^{-1}$
e	x	x	e	e	x
e	y	y	y	y^{-1}	e
y	x	yx	y	y^{-1}	yxy^{-1}
y	y	y^2	y^2	$(y^2)^{-1}$	e
y^2	x	y^2x	y^2	$(y^2)^{-1}$	$y^{-1}xy$
y^2	y	y^3	e	e	e

Table 5.10: *Reidemeister-Schreier scheme for* $G_{3,2} \leq \Gamma$.

where s_1 corresponds to x, s_2 to $xyxy^{-1}x$ and s_3 to $xy^{-1}xy$. The conjugated generators with inverses, H, are, then,

$$g_1 = g_1^{-1} = ps_1^{-1}p^{-1} := \begin{pmatrix} -5i/4 & -3i/4 \\ 3i/4 & 5i/4 \end{pmatrix},$$
$$g_2 = g_2^{-1} = ps_2p^{-1} := \begin{pmatrix} -3i/2 & 1-i/2 \\ 1+i/2 & 3i/2 \end{pmatrix},$$
$$g_3 = ps_3p^{-1} := \begin{pmatrix} 3/2-3i/4 & -1/2-5i/4 \\ -1/2+5i/4 & 3/2+3i/4 \end{pmatrix}, \text{ and}$$
$$g_3^{-1} := \begin{pmatrix} 3/2+3i/4 & 1/2+5i/4 \\ 1/2-5i/4 & 3/2-3i/4 \end{pmatrix}.$$

We use these generators for our computation, and their isometric circles and normalised boundary $U = (g_3,\ g_1,\ g_2)$ are displayed in Figure 5.5a. The reductions of elements in H are then performed in Table 5.11, yielding the new element g_4. This gives rise to the new normalised boundary $U = (g_3,\ g_1,\ g_2,\ g_4)$, displayed in Figure 5.5b. Then, the same reductions are received and we proceed to the pairing of vertices, where g_2 pairs the side $[x_2, x_3]$ with $[x_3, x_2]$. The reductions on the unpaired vertices v_5, x_1 and

g	$\mathrm{red}_{H\setminus\{g\}}(g)$
g_1	g_1
g_2	$g_4 := \begin{pmatrix} 1-3i/4 & 3i/4 \\ -3i/4 & 1+3i/4 \end{pmatrix}$
g_3	e
g_3^{-1}	e

Table 5.11: *$G_{3,2}$: Reductions of elements in step 3, iteration 1.*

v_{10} are shown in Table 5.12. As always, the ideal vertices v_5 and v_{10} are approximated as the intersection of their isometric circles with $|z| = \sqrt{97/100}$.

g	v	$\mathrm{red}_H(g; v_{num})$
g_3	v_5	$g_5 := \begin{pmatrix} 3-3i & -4-i \\ -4+i & 3+3i \end{pmatrix}$
g_1	x_1	$g_6 := \begin{pmatrix} 3/2+9i/4 & 5/2-i/4 \\ 5/2+i/4 & 3/2-9i/4 \end{pmatrix}$
g_3	x_1	g_6
g_4	v_{10}	g_4x

Table 5.12: *$G_{3,2}$: Reductions on vertices in step 5, iteration 1.*

Thus, the new exterior domain, with the normalised boundary

$$U = (g_5,\ g_3,\ g_6,\ g_1,\ g_2,\ g_4)$$

is shown in Figure 5.5c. In the reduction step in step 3 nothing new appears, so we move straight along to a new pairing check. Still, the only paired vertices are x_2 and x_3, so we make reductions on the unpaired vertices $v_{11},\ x_4,\ x_5,\ x_6$ and v_{10}. They are shown in Table 5.13. The new exterior

g	v	$\mathrm{red}_H(g; v_{num})$
g_5	v_{11}	$g_7 := \begin{pmatrix} 3 & -2-2i \\ -2+2i & 3 \end{pmatrix}$
g_5	x_4	$g_8 := \begin{pmatrix} -3/2+5i/4 & 3/2+3i/4 \\ 3/2-3i/4 & -3/2-5i/4 \end{pmatrix}$
g_3	x_4	g_8
g_3	x_5	$g_9 := \begin{pmatrix} -3i/2 & -1-i/2 \\ -1+i/2 & 3i/2 \end{pmatrix}$
g_6	x_5	g_6
g_6	x_6	g_6
g_1	x_6	g_3
g_4	v_{10}	g_4

Table 5.13: *$G_{3,2}$: Reductions on vertices in step 5, iteration 2.*

domain with normalised boundary $U = (g_7,\ g_8,\ g_3,\ g_9,\ g_1,\ g_2,\ g_4)$ is shown in Figure 5.5d.

There are no new reductions in step 3 and in the final step we find the side-pairings $g_1([x_{10}, x_2]) = [x_2, x_{10}]$, $g_2([x_2, x_3]) = [x_3, x_2]$ and $g_9([x_9, x_{10}]) = [x_{10}, x_9]$. Thus, the reductions on unpaired vertices $v_{15},\ x_7,\ x_8$ and v_{10} are displayed in Table 5.14.

g	v	$\mathrm{red}_H(g; v_{num})$
g_7	v_{15}	$g_{10} := \begin{pmatrix} -3/2-23i/4 & -9/2+15i/4 \\ -9/2-15i/4 & -3/2+23i/4 \end{pmatrix}$
g_7	x_7	$g_4^{-1} := \begin{pmatrix} -1-3i/4 & 3i/4 \\ -3i/4 & -1+3i/4 \end{pmatrix}$
g_8	x_7	g_4^{-1}
g_8	x_8	g_4^{-1}
g_3	x_8	g_4^{-1}
g_4	v_{10}	g_4

Table 5.14: *$G_{3,2}$: Reductions on vertices in step 5, iteration 3.*

The new normalised boundary $U = (g_4^{-1},\ g_9,\ g_1,\ g_2,\ g_4)$, together with the isometric circles, is displayed in Figure 5.5e. This is a side-pairing, according to

$$g_1([x_{10}, x_2]) = [x_2, x_{10}], \qquad g_2([x_2, x_3]) = [x_3, x_2],$$
$$g_4([x_3, v_{10}]) = [x_9, v_{21}], \qquad g_9([x_9, x_{10}]) = [x_{10}, x_9],$$

displayed in Figure 5.5f, with added mid-vertices for the elements of order 2.

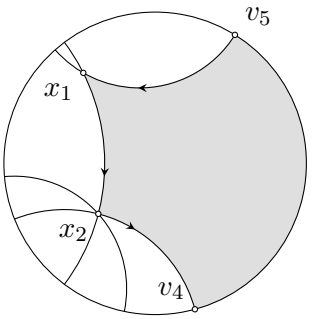

(a) *The isometric circles of* g_1, g_2, g_3 *and* g_3^{-1} *and their exterior domain with normalised boundary.*

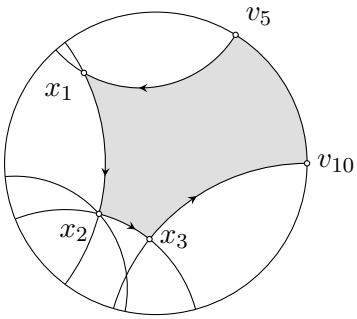

(b) *The isometric circles of* g_1, g_2, g_3, g_3^{-1} *and* g_4 *and their exterior domain with normalised boundary.*

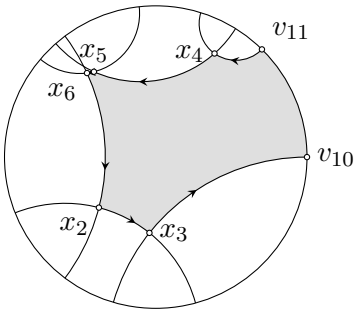

(c) *The isometric circles of* g_1, g_2, g_3, g_4, g_5 *and* g_6 *and their exterior domain with normalised boundary.*

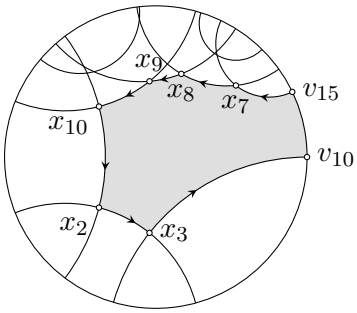

(d) *The isometric circles of* g_1, g_2, g_3, g_4, g_5, g_6, g_7, g_8 *and* g_9 *and their exterior domain with normalised boundary.*

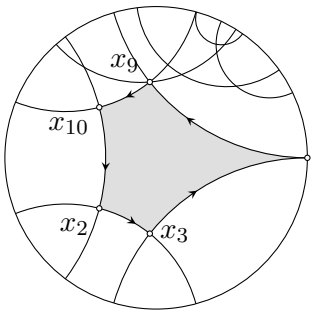

(e) *The isometric circles of* g_1, g_2, g_3, g_4, g_5, g_6, g_7, g_8, g_9, g_{10} *and* g_4^{-1} *and their exterior domain with normalised boundary.*

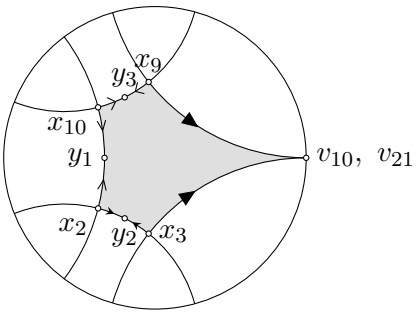

(f) *The isometric circles of* g_1, g_2, g_4, g_9 *and* g_4^{-1} *and the fundamental domain with side-pairing.*

Figure 5.5: *Algorithmic computation for* $G_{3,2}$*, all figures.*

5.5 A Principal Congruence Subgroup of Γ

As an end to our exposé of fundamental domains, we present a special subgroup of Γ, Γ(2). This group can be defined in several ways and has many interesting properties. The most straightforward way is to introduce it via modulo arithmetic, as done by, among others, Jones & Singerman [13, p. 300f]. For any n, the principal congruence subgroup $\Gamma(n) \leq \Gamma$ is the set of elements

$$g = \begin{pmatrix} a & b \\ c & d \end{pmatrix},\ a,\ b,\ c,\ d \in \mathbb{Z},\ \text{such that } g \equiv \begin{pmatrix} \pm 1 & 0 \\ 0 & \pm 1 \end{pmatrix} \mod n.$$

In the case of $n = 2$, the condition is equivalent to $a,\ d$ being odd and $b,\ c$ being even.

The epimorphism which yields the principal congruence subgroup Γ(2) via Singerman's theorem is the following.

$$\begin{aligned} \theta(x) &= (1,4)(3,2)(5,6), & \theta(y) &= (1,3,5)(2,4,6), \\ \theta(y^2) &= (1,5,3)(2,6,4), & \theta(xy) &= (1,2)(3,6)(4,5), \\ \theta(yx) &= (1,6)(2,5)(3,4). \end{aligned}$$

Then $\theta^{-1}(\mathrm{Stab}_{\Sigma_6}(1)) = \Gamma(2)$. This gives us a signature $(g'; -; 3)$, with $g' = 0$ from Riemann-Hurwitz. Using algebra software, see Appendix A.4, we find the right coset representatives of Γ(2) in Γ, satisfying the Schreier condition, as e, x, y, y^2, xy, yx. Thus, we find the generators with the Reidemeister-Schreier scheme in Table 5.15. This means that the generators, expressed

R	P	RP	$\overline{R}$	$\overline{R}^{-1}$	$RP\overline{R}^{-1}$
e	x	x	x	x	e
e	y	y	y	y^2	e
x	x	e	e	e	e
x	y	xy	xy	y^2x	e
y	x	yx	yx	xy^2	e
y	y	y^2	y^2	y	e
y^2	x	y^2x	xy	y^2x	$(y^2x)^2$
y^2	y	e	e	e	e
xy	x	xyx	y^2	y	$(xy)^2$
xy	y	xy^2	yx	xy^2	$(xy^2)^2$
yx	x	y	y	y^2	e
yx	y	yxy	x	x	$(yx)^2$

Table 5.15: *Reidemeister-Schreier scheme for* $\Gamma(2) \leq \Gamma$.

as functions, are $s_1(z) = z + 2$, and $s_2(z) = 1/(2z + 1)$ with the other two generators, being the inverses of s_1 and s_2. The conjugated generators,

together with inverses, are then, in matrix form,

$$g_1 = \begin{pmatrix} 1+i/2 & -i/2 \\ i/2 & 1-i/2 \end{pmatrix}, \qquad g_2 = \begin{pmatrix} 1-2i & -2i \\ 2i & 1+2i \end{pmatrix},$$
$$g_1^{-1} = \begin{pmatrix} 1-i/2 & i/2 \\ -i/2 & 1+i/2 \end{pmatrix}, \text{ and} \qquad g_2^{-1} = \begin{pmatrix} 1+2i & 2i \\ -2i & 1-2i \end{pmatrix}.$$

The isometric circles together with normalised boundary are displayed in Figure 5.6a and since there are no reductions in step 3 and we have a side-pairing in step 5 as $g_1([v_1, v_2]) = [v_4, v_3]$ and $g_2([v_5, v_6]) = [v_8, v_7]$, with their inverses in the opposite direction, all vertices are paired and the fundamental domain is displayed in Figure 5.6b.

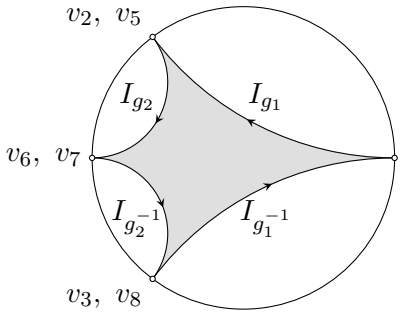

(a) *The isometric circles of g_1, g_1^{-1}, g_2 and g_2^{-1} and their exterior domain with normalised boundary.*

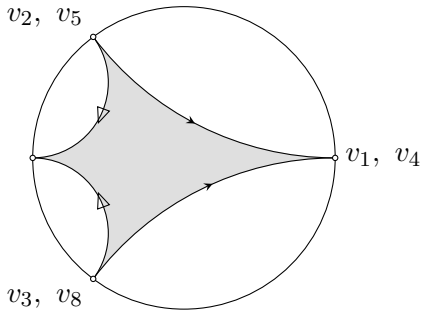

(b) *The isometric circles of g_1, g_1^{-1}, g_2 and g_2^{-1} and the fundamental domain with side-pairing.*

Figure 5.6: *Algorithmic computation for $\Gamma(2)$, all figures.*

Chapter 6

Discussion

We have given an exposition of some methods to help in the study of the important and interesting area of fundamental polygons. The combinatorial methods of Singerman and Reidemeister-Schreier can thus be used to give a starting point for the algorithmic computation of Dirichlet/Ford domains from the generators of the group. This provides a unified way to go from certain cofinite Fuchsian groups to get the Dirichlet/Ford domain for its subgroups of a given index. Since we already get a new domain from the implicit conditions of Singerman's theorem, a legitimate question is what is the real gain to be had from such an extensive approach. First of all, there is the question of explicit generators, which we get from the Reidemeister-Schreier method, and secondly we do not know what type of domain we get from the implicit conditions. It is certainly not necessary that it is a Dirichlet domain, whereas the transfer to a Dirichlet domain is guaranteed by this method in the case of cofinite groups. Moreover, the algorithmic approach opens up the possibility of automation and can thus aid in raising new types of questions that can be asked by allowing a faster construction of fundamental domains and making the process less *ad hoc*.

Some things have been glossed over, in order not to burden the exposition, but as an elucidation of the previous paragraph we make some remarks. For instance, we have not touched upon the fundamental group, even though its connection to the side-pairing of a polygon is intimate. A brief introduction is due. To start with, *path homotopy* is the continuous transformation of two curves with the same end-points into each other while keeping the end-points fixed. Moreover, we are able to invert, by taking the curve in opposite direction, and adjoin curves, by letting one curve $\gamma : [0, 1] \to X$ be immediately followed by another curve $\delta : [0, 1] \to X$ with $\gamma(1) = \delta(0)$. The fundamental group is based at a regular point (not a branch-point) of the space, x_0. Curves both starting and ending at x_0 can either be transformed into each other by path homotopy or not. This divides the set of all curves into equivalence classes, which under adjoining and inverse acts as a group,

known as the *fundamental group*. See [15, Chapter 9].

Moreover, due to the branched covering, we are in reality working with something called *orbifolds* and *orbifold coverings*, which are a generalisation of the concept of manifold, by making the neighbourhood of each point homeomorphic to a *quotient* of a neighbourhood of $\mathbb{R}^n$. Topologically, they are the same, but orbifolds do not have a geometric structure in precisely the same sense as manifolds, due to the existence of branch-points. Outside these points an orbifold acts as a manifold. Recall in this context Figure 2.3b, which is really a quotient map $p : \mathfrak{D} \to \mathfrak{D}/\mathbb{Z}^3$, whereas regular points have a trivial quotient group. See [19, p. 185f]. Moreover, the orbifold has as its fundamental group, in an isomorphic sense, the Fuchsian group, which has now been made explicit in terms of its generators and the side-pairing of the Dirichlet domain. Thus, we get the entire geometry of the orbifold from the fundamental polygon, together with a presentation for its fundamental group: the Fuchsian group.

6.1 Suggestions for Further Study

A number of areas have opened themselves up for further study. There is perhaps a possibility to loosen some of the requirements of Voight's algorithm in Section 4.3, so that reduction need not be done on the isometric circle, but perhaps only outside the exterior domain. Moreover, it would be interesting to think about the problem of hyperbolic boundary elements in this regard, since the algorithm at this point only works for cofinite groups.

In terms of implementation of the algorithm, there is currently some thought going into some form of visualisation software to take advantage of the methods presented and make them more accessible to larger parts of the community. This could, for instance, be used to look for patterns in the fundamental domains of subgroups of the modular group or to see what happens when the centre of the Dirichlet domain is shifted.

Some other directions of investigation would be discrete subgroups of $\mathrm{PSL}(2, \mathbb{C})$. As the reader will recall from Section 4.1, the Ford domain is not limited to Fuchsian groups, but can be used for such *Kleinian groups* as well.

Another direction, where there has been some progress in later years, due to Paul Watson and David Singerman, is in the area of NEC groups, which are discrete groups of isometries, i.e., generalisations of Fuchsian groups, allowing orientation-reversing elements. This is still unpublished research, but a pre-print can be found in [18].

Finally, in 2013, Jane Gilman presented an outline of an algorithm to eliminate generators and relations to give a better homological basis for conformal automorphism groups of Riemann surfaces using the Reidemeister-Schreier method. See [11, p. 137-153].

Appendix A

Code Transcripts

In the appendix, we display transcripts of C++ functions and GAP computations.

A.1 Common C++ Functions

Displayed below are the C++ functions that were used by both functions. Common was also the usage of the symbolic computation library GiNaC.

```
#include <iostream>
#include "ginac/ginac.h"

using namespace std;
using namespace GiNaC;

matrix twoInv(matrix M)
{
  matrix MInv(2,2);
  MInv = M(1,1),-M(0,1),-M(1,0),M(0,0);
  MInv = MInv.mul_scalar(1/M.determinant());
  return MInv;
}

const symbol z("z");
const numeric p = 2*I;
const matrix UH2D(2,2,lst(1,-p,1,-conjugate(p)));
const matrix D2UH = twoInv(UH2D);

numeric conjugate(numeric x)
{
  return real(x) - I*imag(x);
```

```
}

numeric phypdist(numeric z1, numeric z2)
{
  return
  log((abs(z1-conjugate(z2))+abs(z1-z2))/
      (abs(z1-conjugate(z2))-abs(z1-z2)));
}

// Calculate the hyperbolic distance between z1
// and z2 in the unit disc model.
numeric dhypdist(numeric z1, numeric z2)
{
  numeric hz1 = (conjugate(p)*z1-p)/(z1-1);
  numeric hz2 = (conjugate(p)*z2-p)/(z2-1);
  return phypdist(hz1,hz2);
}

ex matToFn(matrix M)
{
  return (M(0,0)*z+M(0,1))/(M(1,0)*z+M(1,1));
}

numeric redmap(const matrix& m, const numeric& n)
{
  ex f = matToFn(m).subs(z == n);
  if (is_a<numeric>(f))
      return dhypdist(ex_to<numeric>(f),numeric(0));
  else
      cerr << "redmap: evaluation failed!" << endl;
}

matrix compose(const matrix& m1, const matrix& m2)
{
  return m1.mul(m2);
}

numeric applyMat(const matrix& m, const numeric& n)
{
  return ex_to<numeric>(matToFn(m).subs(z==n));
}

matrix plane2discmatrix(const matrix& m)
{
```

```
  return compose(UH2D,compose(m,D2UH));
}

matrix disc2planematrix(const matrix& m)
{
  return compose(D2UH,compose(m,UH2D));
}
```

A.2 Computing the Reduction Map in C++

The following displays the code used to implement Algorithm 4.3, with example values for the incoming elements and reduction point.

```
int main()
{
  matrix reduceThisMatrix(2,2);
  numeric reduceWRTPoint(.52-.84*I); // The reduction point.
  vector<pair<matrix,numeric>> setElements;
  matrix setMatrix1(2,2);
  matrix setMatrix1i(2,2);
  matrix setMatrix2(2,2);
  matrix setMatrix2i(2,2);
  setMatrix1 = plane2discmatrix(matrix(2,2,lst(0,-1,1,1)));
  setMatrix1i = twoInv(setMatrix1);
  setMatrix2 = plane2discmatrix(matrix(2,2,lst(1,-1,1,0)));
  setMatrix2i = twoInv(setMatrix2);
  reduceThisMatrix = setMatrix1;
  cout << "gamma = " << reduceThisMatrix << endl;

  setElements.push_back(pair<matrix,numeric>(setMatrix2,0));
  setElements.push_back(pair<matrix,numeric>(setMatrix1i,0));
  setElements.push_back(pair<matrix,numeric>(setMatrix2i,0));
  matrix reducedMatrix(2,2);
  reducedMatrix = reduceThisMatrix;
  matrix reductionMatrix(2,2);
  reductionMatrix = 1,0,0,1;
  numeric r, r_iMin;
  matrix g(2,2);
  do {
    r = redmap(reducedMatrix,reduceWRTPoint);
    cout << "r = " << r << endl;
    r_iMin = pow(numeric(10),numeric(60));
    for (auto it : setElements) {
      it.second = redmap(compose(it.first,reducedMatrix),
```

```
                          reduceWRTPoint);
      if (it.second < r_iMin) {
        g = it.first;
        r_iMin = it.second;
      }
    }
    if (r > r_iMin) {
      reducedMatrix = compose(g,reducedMatrix);
      reductionMatrix = compose(g,reductionMatrix);
      cout << "g = " << g << endl;
      cout << "gGamma = " << reducedMatrix << endl;
      cout << "gDelta = " << reductionMatrix << endl;
    }
  } while (r > r_iMin);
  cout << "red_G(gamma; " << reduceWRTPoint << ") = "
       << reducedMatrix << ", delta = "
       << reductionMatrix << endl;
  return 0;
}
```

A.3 Displaying Vertex Pairings in C++

This is an example of displaying possible vertex pairings, where `V` is the set of vertices under scrutiny and `G` the set of possible pairing elements.

```
int main()
{
  vector<matrix> G;
  list<numeric> V;
  G.push_back(matrix(2,2,lst((1+I/2), -I/2, I/2, (1-I/2))));
  G.push_back(matrix(2,2,lst((numeric(1,2)-I), -numeric(1,2),
                             -numeric(1,2),(numeric(1,2)+I))));
  G.push_back(matrix(2,2,lst((1-I/2), I/2, -I/2,(1+I/2))));
  G.push_back(matrix(2,2,lst((numeric(1,2)+I), numeric(1,2),
                             numeric(1,2),(numeric(1,2)-I))));
  G.push_back(matrix(2,2,lst(-I,0,0,I)));
  G.push_back(matrix(2,2,lst(I,0,0,-I)));
  V.push_back(numeric(3,5)+4*I/5);
  V.push_back(-1);
  V.push_back(I*(sqrt(3)-2));
  V.push_back(1);

  for (auto v : V)
    for (auto g : G)
```

```
      cout << "v : " << v << "\t g : " << g << "\t g(v) : "
           << ex_to<numeric>(matToFn(g).subs(z == v)) << endl;
  return 0;
}
```

A.4 Computing Right Cosets in GAP

The output from GAP, see [6], when computing the Schreier representatives of the right cosets of $H := \mathrm{Stab}_{\Sigma_6}(1)$ in Σ_6. We know that $(1, n)$ gives different cosets for $n = 2, 3, 4, 5, 6$, and find appropriate coset representatives by finding in which coset the images of the words x, y and so on are.

```
gap> G := Group((1,2),(1,3),(1,4),(1,5),(1,6),(2,3),(2,4),(2,5),
                (2,6),(3,4),(3,5),(3,6),(4,5),(4,6),(5,6));
Group([ (1,2), (1,3), (1,4), (1,5), (1,6), (2,3), (2,4), (2,5),
        (2,6), (3,4), (3,5), (3,6), (4,5), (4,6), (5,6) ])
gap> H := Stabilizer(G,1);
Group([ (2,3), (2,4), (2,5), (2,6), (3,4), (3,5), (3,6), (4,5),
        (4,6), (5,6)  ])
gap> one := RightCoset(H,());
RightCoset(Group( [ (2,3), (2,4), (2,5), (2,6), (3,4), (3,5),
                    (3,6), (4,5), (4,6), (5,6) ] ),())
gap> two := RightCoset(H,(1,2));
RightCoset(Group( [ (2,3), (2,4), (2,5), (2,6), (3,4), (3,5),
                    (3,6), (4,5), (4,6), (5,6) ] ),(1,2))
gap> three := RightCoset(H,(1,3));
RightCoset(Group( [ (2,3), (2,4), (2,5), (2,6), (3,4), (3,5),
                    (3,6), (4,5), (4,6), (5,6) ] ),(1,3))
gap> four := RightCoset(H,(1,4));
RightCoset(Group( [ (2,3), (2,4), (2,5), (2,6), (3,4), (3,5),
                    (3,6), (4,5), (4,6), (5,6) ] ),(1,4))
gap> five := RightCoset(H,(1,5));
RightCoset(Group( [ (2,3), (2,4), (2,5), (2,6), (3,4), (3,5),
                    (3,6), (4,5), (4,6), (5,6) ] ),(1,5))
gap> six := RightCoset(H,(1,6));
RightCoset(Group( [ (2,3), (2,4), (2,5), (2,6), (3,4), (3,5),
                    (3,6), (4,5), (4,6), (5,6) ] ),(1,6))
gap> (1,4)(3,2)(5,6) in one;
false
gap> (1,4)(3,2)(5,6) in two;
false
gap> (1,4)(3,2)(5,6) in three;
false
gap> (1,4)(3,2)(5,6) in four;
```

```
true
gap> (1,3,5)(2,4,6) in one;
false
gap> (1,3,5)(2,4,6) in two;
false
gap> (1,3,5)(2,4,6) in three;
true
gap> (1,5,3)(2,6,4) in one;
false
gap> (1,5,3)(2,6,4) in two;
false
gap> (1,5,3)(2,6,4) in three;
false
gap> (1,5,3)(2,6,4) in four;
false
gap> (1,5,3)(2,6,4) in five;
true
gap> (1,2)(3,6)(4,5) in one;
false
gap> (1,2)(3,6)(4,5) in two;
true
gap> (1,6)(2,5)(3,4) in one;
false
gap> (1,6)(2,5)(3,4) in two;
false
gap> (1,6)(2,5)(3,4) in three;
false
gap> (1,6)(2,5)(3,4) in four;
false
gap> (1,6)(2,5)(3,4) in five;
false
gap> (1,6)(2,5)(3,4) in six;
true
```

Thus, a set of coset representatives of H, that in the pre-image satisfies Schreier's condition, are $\theta(e)$ for the stabiliser itself, $\theta(x)$ for $H \cdot (1,4)$, $\theta(y)$ for $H \cdot (1,3)$, $\theta(y^2)$ for $H \cdot (1,5)$, $\theta(xy)$ for $H \cdot (1,2)$ and $\theta(yx)$ for $H \cdot (1,6)$. This means that e, x, y, y^2, xy, yx are representatives of the cosets of $\Gamma(2)$ in Γ.

Remark A.1. The reason we test through from the beginning is to see if we have arrived at the same coset by some previous element of Σ_6 or if the element is in fact in the stabiliser subgroup.

Bibliography

[1] G. Bartolini. *On the Branch Loci of Moduli Spaces of Riemann Surfaces*. Ph.D. Thesis, Linköpings Universitet, 2012.

[2] A. F. Beardon. *The Geometry of Discrete Groups*. Springer-Verlag, New York, 1995.

[3] C. B. Boyer. *A History of Mathematics*. Princeton University Press, Princeton, 1985.

[4] H. S. Coxeter and W. O. J. Moser. *Generators and Relations for Discrete Groups*. Springer-Verlag, Berlin, 1984.

[5] L. R. Ford. *Automorphic Functions*. Chelsea Publishing Company, New York, 1951.

[6] GAP. `http://www.gap-system.org`. Last fetched 2015-06-02.

[7] GiNaC is not a CAS. `http://www.ginac.de`. Last fetched 2015-06-02.

[8] P. A. Grillet. *Abstract Algebra, 2nd Edition*. Springer-Verlag, New York, 2007.

[9] Y. Grosman and W. Magnus. *Groups and their graphs.* Anneli Lax New Mathematical Library: 14. Mathematical Association of America, Washington D.C., 1992.

[10] A. Hurwitz. Ueber Riemann'sche Flächen mit gegebenen Verzweigungspunkten. *Mathematische Annalen*, 39(1):1–60, 1891.

[11] M. Izquierdo, S. A. Broughton, A. F. Costa, and R. E. Rodríguez. *Riemann and Klein Surfaces, Automorphisms, Symmetries and Moduli Spaces (Contemporary Mathematics)*. American Mathematical Society, 2014.

[12] M. Izquierdo and D. Ying. Equisymmetric strata of the moduli space of cyclic trigonal Riemann surfaces of genus 4. *Glasgow Mathematical Journal*, 51(1):19–29, 2009.

[13] G. A. Jones and D. Singerman. *Complex Functions: An Algebraic and Geometric Viewpoint*. Cambridge University Press, Cambridge, 1987.

[14] W. S. Massey. *Algebraic Topology: An Introduction*. Springer-Verlag, New York, 1990.

[15] J. R. Munkres. *Topology. Pearson New International Edition*. Pearson Education Limited, Harlow, 2013.

[16] H. Poincaré. *The Foundations of Science: Science and Hypothesis, The Value of Science, Science and Method*. Project Gutenberg, `http://www.gutenberg.org/files/39713/39713-h/39713-h.htm`, 2012. Translated by G.B. Halsted.

[17] D. Singerman. Subgroups of Fuchsian groups and finite permutation groups. *Bulletin of the London Mathematical Society*, 2(3):319–323, 1970.

[18] D. Singerman and P. Watson. Using Hoare's Theorem to find the signature of a subgroup of an NEC group. *Pre-print*, 2014. arXiv:1408.0127 [math.GR].

[19] J. Stillwell. *Geometry of Surfaces*. Springer-Verlag, New York, 1995.

[20] J. Voight. Computing fundamental domains for Fuchsian groups. *J. Théor. Nombres Bordeaux*, 21(2):469–491, 2009.

[21] Wolfram|Alpha. `http://www.wolframalpha.com`. Last fetched 2015-06-02.

[22] H. Zieschang, E. Vogt, and H.-D. Coldewey. *Surfaces and Planar Discontinuous Groups*. Springer-Verlag, Berlin, 1980.